

# Isotopic, trace element and nutrient characterization of coastal waters from Ubatuba inner shelf area, south-eastern Brazil

P.P. Povinec<sup>a,\*</sup>, J. de Oliveira<sup>b</sup>, E.S. Braga<sup>c</sup>, J.-F. Comanducci<sup>a</sup>, J. Gastaud<sup>a</sup>, M. Groening<sup>d</sup>, I. Levy-Palomo<sup>a</sup>, U. Morgenstern<sup>e</sup>, Z. Top<sup>f</sup>

<sup>a</sup> International Atomic Energy Agency, Marine Environment Laboratories, Monaco

<sup>b</sup> Instituto de Pesquisas Energéticas e Nucleares, Laboratório de Radiometria Ambiental, São Paulo, SP CEP 05508-000, Brazil

<sup>c</sup> Instituto Oceanográfico da Universidade de São Paulo, São Paulo, SP CEP 05508-000, Brazil

<sup>d</sup> International Atomic Energy Agency, Isotope Hydrology Laboratory, Vienna, Austria

<sup>e</sup> Institute of Geological and Nuclear Sciences, Lower Hutt, New Zealand

<sup>f</sup> University of Miami, Rosenstiel School of Oceanography, Miami, FL, USA

Received 11 November 2006; accepted 21 July 2007

Available online 23 August 2007

## Abstract

Stable isotopes, tritium, radium isotopes, radon, trace elements and nutrients data were collected during two sampling campaigns in the Ubatuba coastal area (south-eastern Brazil) with the aim of investigating submarine groundwater discharge (SGD) in the region. The isotopic composition ( $\delta D$ ,  $\delta^{18}O$ ,  $^3H$ ) of submarine waters was characterised by significant variability and heavy isotope enrichment. The stable isotopes and tritium data showed good separation of groundwater and seawater groups. The contribution of groundwater in submarine waters varied from a few % to 17%. Spatial distribution of  $^{222}Rn$  activity concentration in surface seawater revealed changes between 50 and 200 Bq m<sup>-3</sup> which were in opposite relationship with observed salinities. Time series measurements of  $^{222}Rn$  activity concentration in Flamengo Bay (from 1 to 5 kBq m<sup>-3</sup>), obtained by *in situ* underwater gamma-spectrometry showed a negative correlation between the  $^{222}Rn$  activity concentration and tide/salinity. This may be caused by sea level changes as tide effects induce variations of hydraulic gradients, which increase  $^{222}Rn$  concentration during lower sea level, and opposite, during high tides where the  $^{222}Rn$  activity concentration is smaller. The estimated SGD fluxes varied during 22–26 November between 8 and 40 cm d<sup>-1</sup>, with an average value of 21 cm d<sup>-1</sup> (the unit is cm<sup>3</sup>/cm<sup>2</sup> per day). The radium isotopes and nutrient data showed scattered distributions with offshore distance and salinity, which implies that in a complex coast with many small bays and islands, the area has been influenced by local currents and groundwater–seawater mixing. SGD in the Ubatuba area is fed by coastal contaminated groundwater and re-circulated seawater (with small admixtures of groundwater), which claims for potential environmental concern with implications on the management of freshwater resources in the region.

© 2007 Elsevier Ltd. All rights reserved.

**Keywords:** submarine groundwater discharge; groundwater; seawater; river water; rain; stable isotopes;  $\delta D$ ;  $\delta^{18}O$ ; tritium; radium isotopes; radon; nutrients; trace elements; coastal zone; Ubatuba; Brazil

## 1. Introduction

Submarine groundwater discharge (SGD) has recently been shown to be a process of importance for management of fresh

water resources and protection of coastal regions. SGD is generally a widespread, but disperse coastal feature that occurs wherever hydrogeologic gradients enable vertical groundwater transport offshore. Most of SGD occurs as a diffuse seepage and identifying discharge sites or quantifying flux rates across the sediment–water interface has been difficult (Burnett et al., 2006). Estimates of SGD depend strongly on the evaluation technique (Martin et al., 2004). Fluxes of SGD estimated from groundwater flow models are typically one to several

\* Corresponding author. Present address: Comenius University, Faculty of Mathematics, Physics and Informatics, Mlynska dolina F-1, SK-84248 Bratislava, Slovakia.

E-mail address: [povinec@fmph.uniba.sk](mailto:povinec@fmph.uniba.sk) (P.P. Povinec).

orders of magnitude smaller than those measured using field instruments or chemical tracers (Moore, 1996). These differences indicate that meteoric water originating as a recharge to onshore aquifers represents only a fraction of total SGD, with the remainder composed of seawater that is mixed with the shallow porewater (Bokuniewicz, 1992; Burnett et al., 2000; Burnett and Dulaiova, 2003).

Several methods have been developed for measuring the magnitude of the SGD fluxes. Benthic chambers, salinity and temperature measurements, chemical analyses and measurements of a range of isotopic tracers at the aquifer–sea interface helped to estimate local and integrated coastal SGD fluxes (Burnett et al., 2006). Groundwater seepage is usually patchy, diffuse, temporally variable, and difficult to quantify. Specific methods have been developed for simulating seawater–freshwater interactions and seawater intrusion using temporal salinity/temperature variations, tide pumping, wind and wave modelling. For the estimation of SGD flux to the sea, the most frequently used method is based on seepage rate measurements (Bokuniewicz, 1992; Taniguchi et al., 2002), although because of seawater circulation in coastal areas it may not give a realistic value for fresh water input into the sea via SGD. As seepage measurements give information on SGD fluxes on local scale only, isotopic tracers have been applied to estimate integrated SGD fluxes over the coast. Isotopic methods of SGD studies using stable ( $^2\text{H}$ ,  $^{13}\text{C}$ ,  $^{15}\text{N}$ ,  $^{18}\text{O}$ ) as well as radioactive ( $^3\text{H}$ ,  $^{14}\text{C}$ , Ra isotopes, radon) isotopes have recently been developed, and SGD investigations have been carried out in several coastal regions (Moore, 2000; Burnett et al., 2000, 2001a, 2006; De Oliveira et al., 2003, 2005, 2006a,b,c; Aggarwal et al., 2004; Moore and Wilson, 2005; Moore, 2006; Moore and de Oliveira, 2008; Povinec et al., 2006a,b; Weinstein et al., 2006). Especially deuterium and  $^{18}\text{O}$  are effective conservative tracers of mixing processes at the groundwater–seawater interface, because there is clear isotopic distinction between on-shore meteoric groundwater and seawater. When combined with other isotopic tracers in the mixing zone,  $\delta\text{D}$  and  $\delta^{18}\text{O}$  serve as useful indicators of the mixing dynamics.

Radium is an ideal SGD tracer as it is highly enriched in groundwater relative to seawater, behaves conservatively and is relatively easily measured. Four natural radium isotopes ( $^{223}\text{Ra}$ ,  $t_{1/2} = 11.4$  d;  $^{224}\text{Ra}$ ,  $t_{1/2} = 3.66$  d;  $^{226}\text{Ra}$ ,  $t_{1/2} = 1620$  y and  $^{228}\text{Ra}$ ,  $t_{1/2} = 5.75$  y) have been used for the assessment of groundwater discharge and coastal water exchange rates in coastal zones (Moore, 1996, 2000, 2006; Moore and Wilson, 2005; Moore and de Oliveira, 2008). The cycling of Ra in the oceans can be considered as the most interesting phase of radium geochemistry. Two main geochemical characteristics control the production and input of Ra isotopes in coastal areas: the existence of particle-reactive Th isotopes in sediments as direct radiogenic parents, and the vastly different environmental behaviour of Ra in fresh and salt water media (De Oliveira et al., 2006a). As  $^{226}\text{Ra}$  half-life is comparable to the mean ocean circulation time, it should be well mixed in seawater with uniform concentrations along the coast. Close to the

margins or to the sea bottom, deviations from this behaviour can occur, which possibly indicates a groundwater input or fluvial sources. On the other hand, the other three isotopes,  $^{228}\text{Ra}$ ,  $^{224}\text{Ra}$  and  $^{223}\text{Ra}$ , presenting radioisotopes with shorter half-lives, are usually found in higher concentrations closer to the continental margins, and decreasing as a function of the distance offshore. They are highly depleted in ocean basins due to their rapid decay and strong depletion in parent Th isotopes, and they have been used to track diffusion and advection from the coasts.

$^{222}\text{Rn}$  has also been successfully used as a tracer for studying marine and coastal processes, especially in the assessment of SGD in several coastal settings. Radon is a radioactive-conservative tracer and because its concentration in groundwater is several orders of magnitude higher than in seawater, it is an ideal tracer for studying groundwater–seawater interactions.  $^{222}\text{Rn}$  is a direct decay product of  $^{226}\text{Ra}$  from the  $^{238}\text{U}$  natural radioactive chain, and thanks to its short half-life (3.83 d) it is a suitable tracer for studying dynamic systems that are usually found in coastal regions. In the  $^{232}\text{Th}$  natural decay chain there is another radon isotope,  $^{220}\text{Rn}$  (also called thoron), with a shorter half-life (55.6 s).  $^{220}\text{Rn}$  is a decay product of  $^{224}\text{Ra}$ , which further decays to several short-lived daughter products. While  $^{228}\text{Ra}$  ( $^{228}\text{Ac}$ ) from the  $^{232}\text{Th}$  decay chain has been (as a part of the radium quartet, together with  $^{226}\text{Ra}$ ,  $^{223}\text{Ra}$  and  $^{224}\text{Ra}$ ) very often used as a tracer of coastal processes (Moore, 2000; Moore and de Oliveira, 2008),  $^{220}\text{Rn}$  is still waiting for its applications in oceanography. Especially in coastal areas rich in thorium,  $^{220}\text{Rn}$  may be a useful tracer of fast coastal processes. Recently temporal and spatial monitoring of SGD has been possible thanks to new technologies based on the analysis of  $^{222}\text{Rn}$  daughter products emitting either alpha-rays (Burnett et al., 2001b; Burnett and Dulaiova, 2003, 2006; Stieglitz, 2005), or gamma-rays (Povinec et al., 2001; Levy-Palomo et al., 2004; Povinec et al., 2006a,b).

An IAEA Coordinated Research Project (CRP) on “Nuclear and Isotopic Techniques for the Characterisation of SGD in Coastal Zones” has recently been completed. The aim of the CRP was to develop new isotope techniques for studying SGD (Povinec et al., 2006a). In the framework of the CRP two expeditions were carried out in 2002 and 2003 offshore Ubatuba (São Paulo region, Brazil). The expedition in 2003 was a joint IAEA-UNESCO intercomparison exercise with participation of several research groups (manual and continuous seepage measurements, piezometers, electromagnetic probing, stable and radioactive isotopes, radon monitoring). Previous CRP investigations were organized in coastal waters of the south-eastern Sicily which is a typical karstic region, in contrast to the Brazilian coast which is represented by granite rocks. The choice of such geologically different regions (Sicily vs. Brazil) has been based on the strategy, developed in the framework of the IAEA-UNESCO SGD cooperation, to visit and study SGD sites with different geological and hydrological conditions, which could primarily affect SGD in the region (Povinec et al., 2006a; Burnett et al., 2006).

Previous work carried out at the Ubatuba site documented modest fluxes of SGD (De Oliveira et al., 2003, 2005, 2006a,b,c; Teixeira, 2004; Lopes, 2005; Almeida et al., 2006). Contamination of bays with nutrients indicated their possible transport via groundwater, as well as by local currents. In this paper we present and discuss isotopic ( $\delta D$ ,  $\delta^{18}O$ ,  $H^3$ , Ra isotopes,  $^{222}Rn$ ), trace elements and nutrients data obtained from the 2002 and 2003 expeditions, and compare them with similar investigations carried out in the Ubatuba region, as well as in other coastal regions.

## 2. Hydrogeological background

The tropical coastal area in the northernmost part of São Paulo Bight (about 270 km north of São Paulo), comprising a series of small embayments near Ubatuba town was visited during expeditions in August 2002 and November 2003 (Fig. 1). The rainfall regime because of the humid tropical climate and the absence of large river basins in the area is important for the transport of freshwater from the continent to the ocean. The coastal aquifer system can be classified as

a fractured rock aquifer, covered by Pleistocene and Holocene sediments. Groundwater discharge patterns are spatially heterogeneous, with preferential water flow paths through rock fractures.

The main geologic/geomorphologic feature of the Ubatuba coast is the presence of pre-Cambrian granites and migmatites of the mountain chain Serra do Mar (altitudes up to 1000 m). Wave action is the most effective hydrodynamic phenomenon responsible for the bottom sedimentary processes in the coastal area as well as in the adjacent inner continental shelf. The terrestrial input of sediments is strongly dependent on the rainfall regime, leading to a higher contribution of sediments during the summer (November–February) season (Mahiques, 1995). The mean annual rainfall is around 1800 mm, the maximum rainfall rates being observed in February.

Three water masses occur in the area: (1) coastal water (CW), characterized by high temperature ( $>25^\circ C$ ) and low salinity (32–33); (2) tropical water (TW) with intermediate temperature (20–23  $^\circ C$ ) and high salinity ( $\sim 36$ ); and (3) South Atlantic central water (SACW) with low temperature (16–18  $^\circ C$ ) and high salinity (35–36). During the summer,

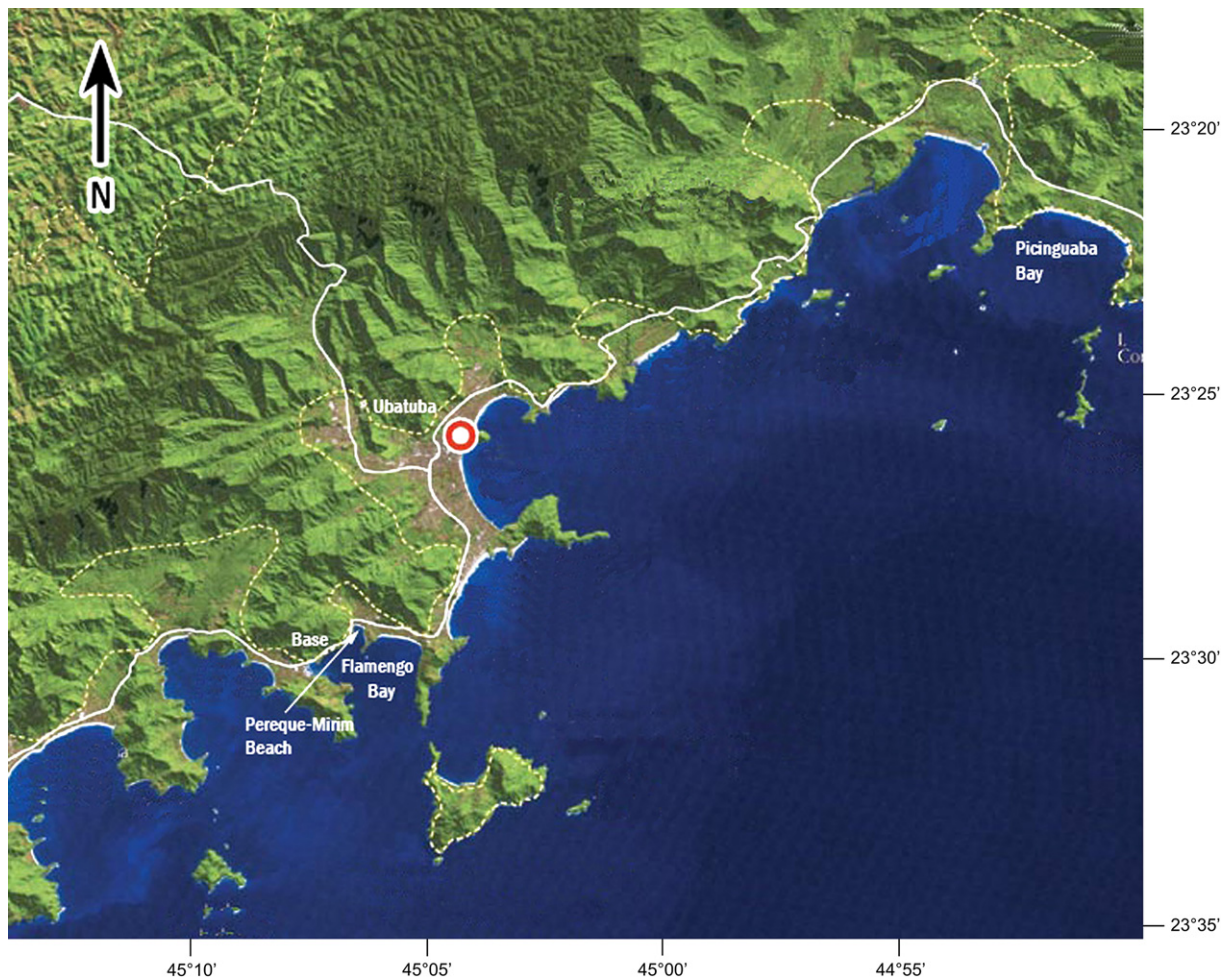


Fig. 1. Ubatuba coast in south-eastern Brazil with typical geologic features. The SGD work was mostly carried out in Flamengo Bay (hosting the Oceanographic Base) and in Pinguaba Bay.

nutrient-rich SACW moves onshore and it is often found in the central and outer portions of the continental shelf (20–100 m), while CW is found along a narrow band inshore. These water movements result in a vertical stratification over the inner shelf, with a strong thermocline at middle depths. In the winter (May through August), when SACW is restricted to the outer shelf, horizontal and vertical thermal gradients are reduced and almost no stratification is observed on the inner shelf (Castro Filho et al., 1987). In summer, the advance of the SACW over the coast leads to the displacement of the CW, rich in continental suspended materials, and to transportation of these sediments to outer portions of the continental shelf. In winter, the retreat of the SACW and the decrease of the rainy levels restrict the input of sediments from continental areas. In Flamengo Bay the sea level varies mostly between 4.4 and 5.5 m, the highest range (4.4–5.9 m) is observed in August–September due to greater volume of warm waters of the Brazil Current (Mesquita, 1997).

### 3. Materials and methods

#### 3.1. Water and sediment samples

Seawater samples were collected during two sampling campaigns (5–15 August 2002 and 14–26 November 2003) in a series of small embayments of Ubatuba using R/Vs Velliger II and Albacora. Surface seawater samples were collected at ~2 m below the sea surface, while bottom samples were collected 1 m above the sea bottom. In 2002, seawater samples were collected in four transects (called A, B, C and T), and in 2003 in three transects (named FB, PB and V), offshore Ubatuba (Fig. 2 and Table 1). Groundwater samples were collected from inland wells and springs situated at the coast facing the Fortaleza, Flamengo and Picinguaba Bays, and at the Vitoria Island. River water samples were collected at the Fazenda beach in Picinguaba Bay, situated north-east of Ubatuba Bay (Fig. 1).

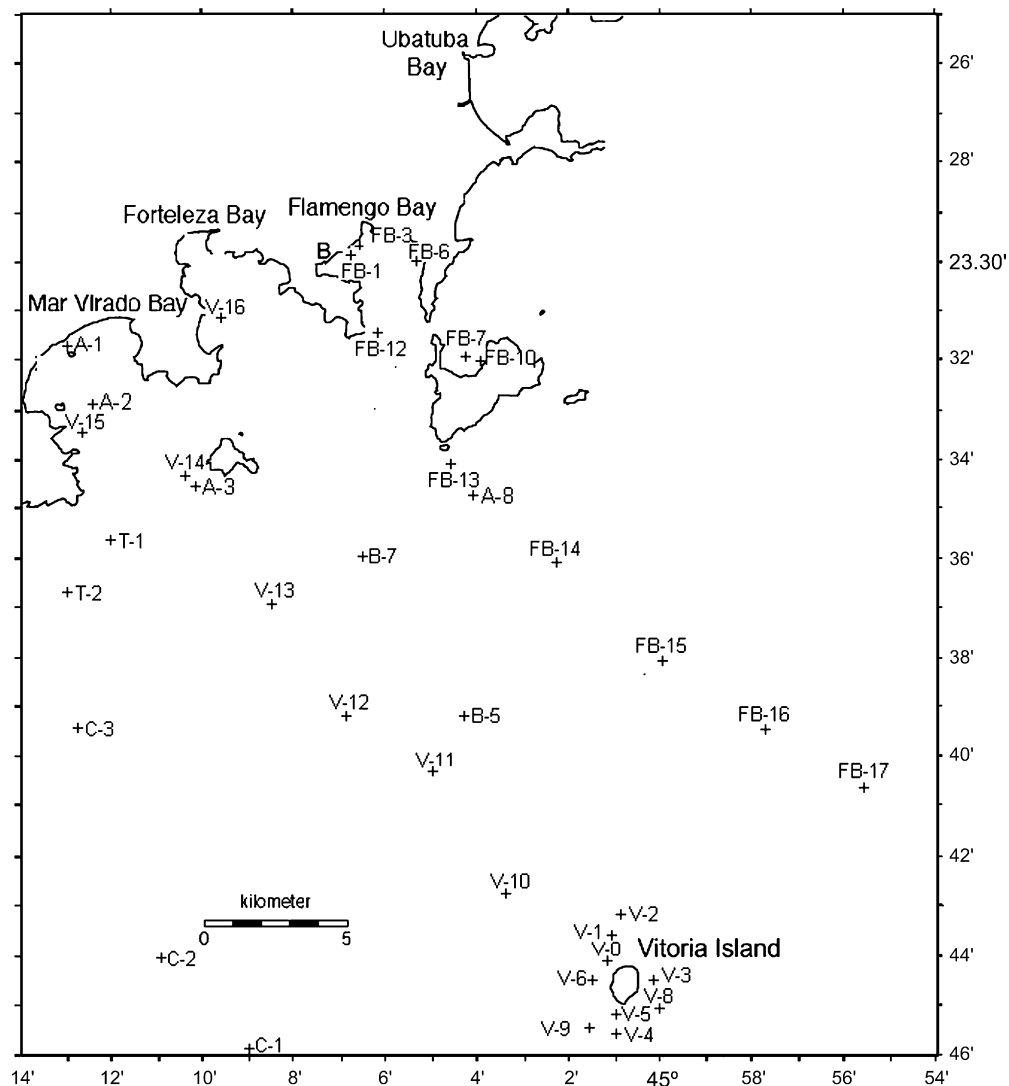


Fig. 2. Sampling sites offshore Ubatuba. Several transects were organised to sample seawater offshore Flamengo, Fortaleza and Mar Virado Bays up to Vitoria Island. The position of the Oceanographic Base (B) in Flamengo Bay is also shown.

Table 1  
Isotope, salinity and temperature data for water samples collected in 2002 and 2003 (for sampling stations see Figs. 2 and 3). GW, groundwater well; GS, groundwater spring; RW, river water; PR, precipitation; PM, borehole well; MS, piezometer multisampler; SD, seepage chamber; LT, low tide; HT, high tide. The precision of  $\delta D$  and  $\delta^{18}O$  at 1 $\sigma$  level was  $\pm 1\text{‰}$  and  $\pm 0.1\text{‰}$ , respectively. The total uncertainty for  $^3H$  measurements is given at the 1 $\sigma$  level

Station	Sample origin	Latitude	Longitude	Date	Water depth (m) <sup>a</sup>	Type	$\delta D$ (‰)	$\delta^{18}O$ (‰)	$^3H$ (TU)	Salinity	$T$ (°C)
<i>Isotope data for August 2002</i>											
<b>Flamengo, Fortaleza and Mar Virado Embayments</b>											
A-1	Transect A	S23°32.052	W45°13.352	8	2	SW	1.2	0.16	1.33 ± 0.21	33.2	21.7
A-1b <sup>b</sup>	Transect A	S23°32.052	W45°13.352	8	5	SW	1.4	0.20	0.96 ± 0.04	33.1	21.6
A-2	Transect A	S23°33.080	W45°12.002	7	7	SW	1.0	0.12	1.34 ± 0.23	33.4	19.9
A-3	Transect A	S23°33.963	W45°10.474	7	12	SW	2.0	0.00	0.97 ± 0.03	33.5	20.8
A-8	Transect A	S23°34.625	W45°04.638	6	17	SW	4.2	0.17	1.48 ± 0.26	34.1	21.0
AB-1-HT	Base	S23°29.952	W45°07.093	9	1	SW	3.2	0.16	2.11 ± 0.29	32.9	22.0
AB-1-LT	Base	S23°29.955	W45°07.090	9	1	SW	2.9	0.20	2.69 ± 0.29	32.8	22.0
<b>Fortaleza and Mar Virado Embayments</b>											
B-5	Transect B	S23°39.110	W45°04.341	6	20	SW	3.2	0.30	0.92 ± 0.04	33.7	21.0
B-7	Transect B	S23°36.220	W45°06.852	6	20	SW	2.7	0.10	0.90 ± 0.04	33.5	21.0
<b>Transect C to São Sebastião Island</b>											
C-0	Transect C	S23°50.234	W45°11.132	8	40	SW	2.0	0.08	1.23 ± 0.20	33.2	20.8
C-0b	Transect C	S23°50.234	W45°11.132	8	40	SW	2.9	0.19	1.16 ± 0.23	33.6	20.7
C-1	Transect C	S23°46.511	W45°09.607	8	32	SW	1.4	0.12	1.01 ± 0.23	33.6	20.7
C-1b	Transect C	S23°46.511	W45°09.607	8	32	SW	4.1	0.26	1.36 ± 0.23	33.5	20.6
C-2	Transect C	S23°44.118	W45°11.208	8	28	SW	4.2	0.10	1.0 ± 0.04	33.6	20.6
C-3	Transect C	S23°39.390	W45°13.248	8	17	SW	1.7	0.0	1.28 ± 0.04	33.0	21.0
C-3b	Transect C	S23°39.390	W45°13.248	8	17	SW	4.5	0.32	1.28 ± 0.26	34.1	21.0
C-4	Transect C	S23°36.443	W45°16.992	7	13	SW	1.6	0.09	1.26 ± 0.04	32.9	20.7
<b>Transect T parallel to the coast line from Fortaleza Bay to São Sebastião Island</b>											
T-1	Transect T	S23°35.422	W45°11.919	7	14	SW	1.7	0.00	1.00 ± 0.03	32.0	21.0
T-2	Transect T	S23°36.572	W45°13.008	7	14	SW	2.1	0.16	1.37 ± 0.27	33.3	20.8
T-2b	Transect T	S23°36.572	W45°13.008	7	14	SW	4.2	0.24	2.34 ± 0.43	33.3	20.8
T-3	Transect T	S23°38.489	W45°15.161	7	14	SW	1.4	0.00	1.11 ± 0.04	34.0	21.0
T-4	Transect T	S23°40.817	W45°17.834	7	15	SW	1.8	0.13	1.40 ± 0.28	34.0	21.4
T-4b	Transect T	S23°40.817	W45°17.834	7	15	SW	2.9	0.30	1.11 ± 0.23	34.0	21.4
T-5	Transect T	S23°43.324	W45°20.498	7	15	SW	1.3	-0.02	1.62 ± 0.24	32.7	21.1
<b>Borehole monitoring wells at Flamengo Bay</b>											
PM-3	Well, LT	S23°31.893	W45°09.891	9	0.90 <sup>c</sup>	GW	-13.1	-3.14	2.99 ± 0.22	0.0	23.0
PM-3	Well, HT	S23°31.893	W45°09.891	9		GW	-14.7	-3.20	2.00 ± 0.05	0.0	23.0
PM-4	Well, LT	S23°31.893	W45°09.891	9	1.80 <sup>c</sup>	SW + GW	2.5	0.00	1.19 ± 0.04	33.1	25.3
PM-4	Well, HT	S23°31.893	W45°09.891	9		SW + GW	2.9	0.40	1.65 ± 0.05	33.1	25.3
PM-7	Well, LT	S23°31.893	W45°09.891	9	2.10 <sup>c</sup>	SW + GW	2.8	0.35	2.06 ± 0.23	29.9	25.2
PM-7	Well, HT	S23°31.893	W45°09.891	9		SW + GW	3.5	0.39	1.64 ± 0.33	29.9	25.2
<b>Groundwater springs, wells and rain water</b>											
GW-1	Corsario	S23°30.547	W45°07.716	5		GW	-12.6	-3.52	2.21 ± 0.20	0.0	
GS-1	Base	S23°30.008	W45°07.118	9		GW	-15.3	-3.73	2.48 ± 0.21	0.0	
GS-2	Road	S23°30.007	W45°07.116	10		GW	-18.3	-3.9	2.05 ± 0.05	0.0	
PR-1	Rain w. (Base)	S23°30.008	W45°07.118	9		PR	-20.0	-3.7	2.52 ± 0.23	0.0	
<i>Isotope data for November 2003</i>											
FB-1	Flamengo Bay <sup>d</sup>	S23°30.030	W45°07.067	18	2	SW	3.3	0.29		33.84	
FB-2	Flamengo Bay	S23°29.938	W45°06.998	18	2	SW	3.2	0.35		33.77	

FB-3	Flamengo Bay	S23°30.000	W45°06.350	18	2	SW	3.4	0.51		33.64	
FB-4	Flamengo Bay	S23°29.295	W45°06.343	18	3	SW	2.6	0.41		33.59	
FB-5	Flamengo Bay	S23°29.392	W45°06.209	18	3	SW	2.6	0.39		33.88	
FB-6	Flamengo Bay	S23°29.734	W45°05.035	18	3	SW	3.1	0.45		33.99	
FB-7	Flamengo Bay	S23°32.124	W45°04.624	18	5	SW	2.9	0.42		34.11	
FB-8	Flamengo Bay	S23°32.155	W45°04.690	18	5	SW	2.9	0.43		34.19	
FB-9	Flamengo Bay	S23°32.194	W45°04.779	18	5	SW	3.4	0.55		34.84	
FB-10	Flamengo Bay	S23°32.234	W45°03.853	18	6	SW	2.5	0.30		34.19	
FB-11	Flamengo Bay	S23°30.008	W45°07.118	18	2	SW	3.2	0.16	2.11 ± 0.29	32.1	
V-0	Vitoria Isl. <sup>c</sup>	S23°44.081	W45°01.390	24	21	SW	3.5	0.51		34.50	24.8
V-1	Vitoria Isl.	S23°43.560	W45°01.200	24	22	SW	3.5	0.53		34.55	24.8
V-2	Vitoria Isl.	S23°43.150	W45°01.054	24	41	SW	3.1	0.44		34.29	24.8
V-3	Vitoria Isl.	S23°44.649	W45°00.562	24	43	SW	3.3	0.42		34.55	24.7
V-4	Vitoria Isl.	S23°45.707	W45°01.085	24	20	SW	3.4	0.53		34.60	24.2
V-5	Vitoria Isl.	S23°45.167	W45°01.106	24	26	SW	2.9	0.40		33.32	24.8
V-6	Vitoria Isl.	S23°44.471	W45°01.505	24	2	SW	3.0	0.39	1.21 ± 0.05	34.23	24.3
PM-1	Well, LT	S23°30.009	W45°07.113	21	5.0 <sup>c</sup>	GW	-9.4	-2.93		0.1	22.8
PM-1	Well, HT	S23°30.009	W45°07.113	21		GW	-10.6	-2.96		0.1	22.8
PM-1	Well, HT	S23°30.009	W45°07.113	25		GW	-10.4	-2.97		0.1	22.8
PM-4	Well, HT	S23°30.013	W45°07.095	21	1.80 <sup>c</sup>	SW + GW	3.8	0.49		34.0	25.3
PM-4	Well, LT	S23°30.013	W45°07.095	25		SW + GW	3.6	0.32		33.4	25.2
PM-5	Well, HT	S23°30.018	W45°07.085	21	2.0 <sup>c</sup>	SW + GW	2.1	0.49		33.6	26.0
PM-5	Well, LT	S23°30.018	W45°07.085	25		SW + GW	2.0	0.47		33.2	25.9
PM-6	Well, LT	S23°29.999	W45°07.107	25	1.50 <sup>c</sup>	GW	-6.4	-2.37		0.1	23.1
PM-6	Well, HT	S23°29.999	W45°07.107	21		GW	-7.0	-2.41		0.1	23.1
PM-6	Well, LT	S23°29.999	W45°07.107	25		GW	-6.8	-2.40		0.1	23.1
PM-7	Well, HT	S23°30.007	W45°07.093	21	2.10 <sup>c</sup>	SW + GW	1.6	0.12		31.5	25.4
PM-8	Well, LT	S23°30.012	W45°07.084	21	1.95 <sup>c</sup>	SW + GW	3.9	0.36		33.4	26.5
MS-4/1 <sup>f</sup>	Piezometer	S23°30.008	W45°07.118	19		SW + GW	3.1	0.35	1.36 ± 0.02	33.6	25.7
MS-4/2	Piezometer	S23°30.008	W45°07.118	19		SW + GW	3.3	0.33		33.2	27.4
MS-4/3	Piezometer	S23°30.008	W45°07.118	19		SW + GW	3.0	0.31		33.2	29.1
MS-4/4	Piezometer	S23°30.008	W45°07.118	19		SW + GW	2.8	0.29		33.2	28.4
MS-4/5	Piezometer	S23°30.008	W45°07.118	19		SW + GW	2.6	0.26		33.0	28.2
MS-4/8	Piezometer	S23°30.008	W45°07.118	19		SW + GW	0.05	0.14	1.05 ± 0.02	32.1	27.5
MS-5/1	Piezometer	S23°30.008	W45°07.118	20		SW + GW	0.06	-0.15		31.9	26.2
MS-5/2	Piezometer	S23°30.008	W45°07.118	20		GW	-11.0	-2.9	1.92 ± 0.03	4.1	25.9
MS-5/3	Piezometer	S23°30.008	W45°07.118	20		GW	-13.1	-0.32		0.5	28.8
MS-5/4	Piezometer	S23°30.008	W45°07.118	20		GW	-13.0	-0.32		1.6	28.8
MS-5/5	Piezometer	S23°30.008	W45°07.118	20		SW + GW	-12.7	-3.25	2.20 ± 0.03	0.4	28.1
SD-1E/1 <sup>g</sup>	Seepage ch. HT	S23°30.008	W45°07.118	18		SW + GW	0.6	-0.05	2.10 ± 0.03	26.2	
SD-1E/3	Seepage ch.	S23°30.008	W45°07.118	18		SW + GW	0.5	-0.03		25.8	
SD-1E/5	Seepage ch.	S23°30.008	W45°07.118	18		SW + GW	0.4	-0.07		25.5	
SD-1E/6	Seepage ch. LT	S23°30.008	W45°07.118	18		SW + GW	0.5	0.0		25.7	
SD-2	Seepage ch. HT	S23°30.008	W45°07.118	19		SW + GW	0.0	-0.22		27.5	
SD-5	Seepage ch. HT	S23°30.548	W45°07.718	19		SW + GW	1.7	0.15		32.3	
FB-1/SS	Flamengo Bay - spectrometer site HT	S23°30.008	W45°07.118	22		SW + GW	0.6	0.2		33.7	
FB-2/SS	Flamengo Bay - spectrometer site HT	S23°30.008	W45°07.118	24		SW + GW	0.5	0.2		33.4	
FB-3/SS	Flamengo Bay - spectrometer site LT	S23°30.008	W45°07.118	25		SW + GW	0.3	0.1		32.9	

(continued on next page)

Station	Sample origin	Latitude	Longitude	Date	Water depth (m) <sup>a</sup>	Type	$\delta D$ (‰)	$\delta^{18}O$ (‰)	$^3H$ (TU)	Salinity	T (°C)
GW-1	Corsario	S23°30.547	W45°07.716	16		GW	-15.5	-3.54		0.0	
GS-1	Base	S23°30.008	W45°07.118	16		GW	-11.2	-3.17	2.61 ± 0.04	0.0	
GS-2	Road	S23°30.007	W45°07.116	26		GW	-13.7	-3.45	2.69 ± 0.04	0.0	
GS-3	Vitoria Isl.	S23°45.046	W45°01.079	24		GW	-16.9	-3.71	2.59 ± 0.04	0.0	
GS-4	Vitoria Isl	S23°45.046	W45°01.095	24		GW	-16.4	-3.62		0.0	
RW-7	Fazenda Beach	S23°29.523	W45°05.387	19		RW	-15.6	-3.61		0.0	
RW-8	Fazenda Beach	S23°21.286	W45°51.844	19		RW	-14.9	-3.57	2.42 ± 0.20	0.0	
RW-9	Fazenda Beach	S23°21.514	W45°51.387	19		RW	-11.6	-3.16		0.1	
RW-10	Fazenda Beach	S23°21.571	W44°51.175	19		RW	-9.3	-2.92		0.7	
RW-12	Fazenda Beach	S23°22.029	W44°50.240	19		RW	-14.0	-3.00		2.6	
PR-2	Rain w. (Base)	S23°30.008	W45°07.118	18		PR	-17.5	-3.5	2.65 ± 0.22	0.0	

<sup>a</sup> Water column depth; surface samples were collected at ~2 m water depth (except the samples collected in shallower waters).

<sup>b</sup> Bottom samples (b) were collected 1 m above the sea bottom.

<sup>c</sup> Wells depth below the sediment surface.

<sup>d</sup> Flamengo Bay transect.

<sup>e</sup> Vitoria Island transect.

<sup>f</sup> Water samples from Cable and Martin, 2008.

<sup>g</sup> Water samples from Bokuniewicz et al., 2008.

For measuring groundwater seepage rates from the sediment, water samples were also collected from seven monitoring borehole wells drilled on the beach at the Oceanography Base of the University of São Paulo at Flamengo Bay (Fig. 3). The well PM-3 was accidentally destroyed in 2003, and well PM-2 was without water in 2002, as well as in 2003. Water samples collected by Cable and Martin (2008) from two piezometer multisampler tubes located between wells PM-6 and PM-8 (MS-5, 6.5 m from the shoreline, Fig. 3) and behind PM-8 (MS-4, 35 m from the shoreline), were also analysed. Porewater was collected from different horizons, between 10 and 230 cm (for MS-4) and 16 and 176 cm (for MS-5) below the sediment surface. Water samples collected by Bokuniewicz et al. (2008) from three manual seepage chambers located at the low tide shoreline (SD-1E), at 5 m from the shoreline (SD-2) and at 32 m from the shoreline (SD-5) were also analysed. The seepage chambers were deployed long enough to be well flushed by groundwater and/or re-circulated seawater. The samples from borehole wells and seepage chambers were collected during both low and high tides. Water samples for isotope and elemental analysis were collected in 1 L polyethylene bottles using submersible pumps (for seawater), or peristaltic pumps (for groundwater). The samples were filtered through 0.45  $\mu$ m glass microfibre filters (Millipore). Water samples for laboratory analysis of nutrients were collected by 250 mL plastic vials that were pre-washed with 0.5 M hydrochloric acid and sample-rinsed three times. Samples were kept frozen until analysis.

Sediment samples were collected at a few seawater stations offshore Ubatuba using a Van Veen grab sampler. The samples were analyzed for  $^{226}\text{Ra}$  and  $^{228}\text{Ra}$  with the aim of checking their availability in sediment, to estimate  $^{222}\text{Rn}$  concentrations emanated from sediments, as well as for calibration of the *in situ* gamma-spectrometer. The locations of all sampling stations and results obtained in August 2002 (winter) and November 2003 (summer) expeditions are given in Tables 1–4.

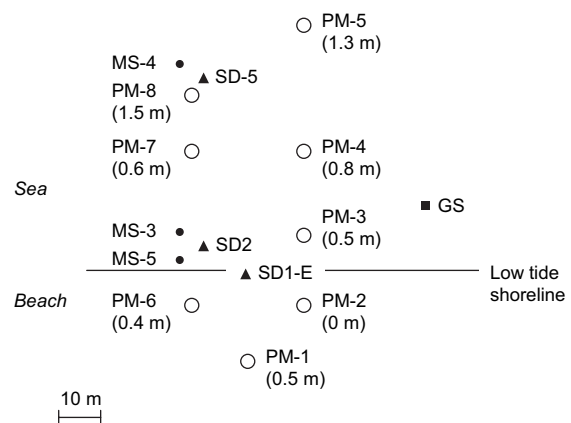


Fig. 3. Monitoring site in Flamengo Bay in front of the Oceanographic Base. Positions of monitoring borehole wells (PM), seepage chambers (SD), piezometer multisamplers (MS) and the underwater gamma-spectrometer (GS) are shown together with the low tide shoreline. Water levels in the wells are shown in brackets.

Table 2

Chlorine and trace element data. A, B, C, T, FB, V, seawater transects; GW, groundwater well; GS, groundwater spring; RW, river water; PM, borehole well; MS, piezometer multi-sampler; SD, seepage chamber; LT, low tide; HT, high tide. The total relative uncertainties are below 1% (at 1 $\sigma$  level)

Station	Sample origin	Sampling date	Cl (mg/g)	S ( $\mu$ g/g)	K ( $\mu$ g/g)	Ca ( $\mu$ g/g)	Br ( $\mu$ g/g)	Sr ( $\mu$ g/g)	Ba ( $\mu$ g/g)
<b>August 2002</b>									
T1	Transect T	7	18.5	780	450	420	83	8.4	5.2
T2	Transect T	7	18.9	808	470	430	84	8.2	4.7
T3	Transect T	7	19.0	810	450	440	84	8.3	8.2
T4	Transect T	7	19.2	810	450	430	84	8.7	4.8
T5	Transect T	7	18.5	790	460	440	82	8.2	4.6
A3	Transect A	7	18.9	780	500	430	82	8.0	4.1
A8	Transect A	6	19.1	810	450	450	85	8.5	4.1
AB-1 HT	Base	6	19.3	780	450	430	84	8.4	4.1
AB-1 LT	Base	9	18.7	710	460	440	83	8.5	4.6
B5	Transect B	6	19.1	810	470	430	83	8.3	7.5
B7	Transect B	6	19.2	800	440	440	85	8.6	6.5
C0	Transect C	8	19.0	800	450	430	85	8.2	5.8
C1	Transect C	8	18.9	790	440	440	84	8.2	4.1
C2	Transect C	8	19.2	810	460	440	85	8.6	4.2
C3	Transect C	8	19.1	810	450	440	86	8.3	4.1
PM-3	Well LT	9	1.15	<10	<10	37	5.2	0.8	4.3
PM-3	Well HT	9	<0.01	<10	<10	<0.5	<0.2	0.6	5.2
PM-7	Well LT	9	19.2	770	450	440	85.3	8.3	4.1
PM-7	Well HT	9	19.3	780	450	430	84.4	8.4	4.1
GW-1	Corsario	5	0.024	<10	<10	5.2	<0.2	<0.2	<1.4
GS-1	Base	5	0.018	<10	<10	<0.5	<0.2	<0.2	4.4
<b>November 2003</b>									
FB-1	Flamengo Bay	18	19130	830	450	450	86	8.3	7.5
FB-2	Flamengo Bay	18	19490	800	480	450	86	8.5	<4
SD-1E/1	Seepage chamber HT	18; 13:12-13:39	15190	630	370	380	68	7.1	<4
SD-1E/2	Seepage chamber	18; 13:39-14:08	15370	640	390	380	68	6.8	7.6
SD-1E/3	Seepage chamber	18; 14:09-14:40	15110	630	380	370	66	6.6	<4
SD-1E/4	Seepage chamber	18; 14:40-15:10	14990	620	360	360	66	6.7	8.1
SD-1E/5	Seepage chamber	18; 15:10-15:42	15240	630	370	370	66	6.9	8.0
SD-1E/6	Seepage chamber LT	18; 15:42-16:04	15210	720	370	390	67	7.0	4.6
MS4-1	Piezometer	19; 12:30	18590	800	440	440	84	7.9	7.0
MS4-2	Piezometer	19; 12:10	18800	800	470	440	84	8.2	9.9
MS4-3	Piezometer	19; 12:00	18740	800	480	430	83	8.3	4.9
MS4-4	Piezometer	19; 11:30	18980	830	480	450	84	8.5	4.7
MS4-5	Piezometer	19; 11:10	18860	810	480	430	83	8.5	4.5
MS4-8	Piezometer	19; 10:20	19080	810	470	440	84	8.4	5.4
MS5-3	Piezometer	20; 10:00	2190	34	52	58	9.7	1.3	<4
MS5-3	Piezometer	20; 11:00	2460	46	51	63	10.5	1.3	<4
MS5-4	Piezometer	20; 11:05	17890	740	430	420	79	7.7	<4
MS5-4	Piezometer	20; 10:50	190	<10	<10	8.5	0.8	0.5	<4
MS5-5	Piezometer	20; 10:45	710	<10	<11	16.0	3.2	0.4	<4
MS5-6	Piezometer	20; 10:15	150	<10	<10	3.5	0.8	0.3	4.1
MS5-7	Piezometer	20; 10:05	200	<10	<10	3.1	0.9	0.4	<4
PM-1 LT	Well	21	<1.2	<10	<10	5.5	0.4	0.4	<4
PM-1 HT	Well	21	72	<1.0	<11	8.1	0.3	0.3	6.4
PM-4 HT	Well	21	19460	830	480	450	86	8.5	3.5
PM-5 HT	Well	21	19640	810	480	450	87	8.5	<4
PM-6 HT	Well	21	<1.3	<10	<10	140	<0.2	0.4	<4
PM-7 HT	Well	21	18250	750	420	450	81	8.4	4.5
PM-8 LT	Well	21	19690	830	480	460	86	8.9	4.7
PM-1 LT	Well	25	65	<10	<10	7.1	0.4	0.3	<4
PM-1 HT	Well	25	72	<10	<10	9.6	0.3	0.4	4.0
PM-6 LT	Well	25	<1.3	<10	<10	14.5	<0.1	0.4	<4
PM-4 LT	Well	25	19230	800	480	440	85	8.6	5.2
PM-7 LT	Well	25	18030	740	430	430	79	7.9	4.2

(continued on next page)

Table 2 (continued)

Station	Sample origin	Sampling date	Cl (mg/g)	S (μg/g)	K (μg/g)	Ca (μg/g)	Br (μg/g)	Sr (μg/g)	Ba (μg/g)
RW-2	Pereque Beach	19	<1.2	<10	<10	14.4	<0.1	0.3	4.4
RW-3	Pereque Beach	19	10.0	<10	<10	21.5	0.2	0.4	6.7
RW-5	Enseada Beach	19	<1.2	<10	<9.9	10.7	<0.1	0.3	4.6
GS-1	Base	18	<1.3	<10	<11	<1.1	<0.1	0.4	5.4
GS-2	Road	16	<1.2	<10	<10	1.4	<0.1	0.4	<4
GS-3	Vitoria Isl.	24	22	<10	<10	<1.1	<0.2	0.5	<4
GS-4	Vitoria Isl.	24	24	<1.0	<10	<1.1	<0.2	0.3	6.1

### 3.2. Salinity and temperature measurements

Salinity at visited sites was continuously measured *in situ* using a 2' Micro-CTD (Falmouth Scientific Inc., USA) with precision of  $\pm 0.001$ . Temporal variations of salinity in monitoring borehole wells were measured continuously by a small “fish” DST-CTD sensor (Star-Oddi, Iceland) with precision of  $\pm 0.01$ . Conductivity/salinity and temperature measurements in the field and in the laboratory were done using portable meters. A seawater standard (Oceanor Scientific Instruments Atlantic Sea Water 35) was used for inter-instrument salinity calibrations.

### 3.3. Analysis of trace elements

Trace elements in water samples were analysed by IAEA-MEL using the XRF method (Povinec et al., 2002). The total relative uncertainties were below 1% (at  $1\sigma$  level). Reference samples produced by IAEA were analysed simultaneously with collected samples.

### 3.4. Analysis of stable isotopes

Isotopic analyses were carried out on groundwater and seawater samples.  $\delta^{18}\text{O}$  analyses were performed using the  $\text{CO}_2$ –

$\text{H}_2\text{O}$  equilibration procedure reported in Epstein and Mayeda (1953).  $\delta\text{D}$  analyses were done using  $\text{H}_2\text{O}$ –Zn reduction (Coleman et al., 1982). The isotopic results were reported against the international standard VSMOW (Vienna Standard Mean Ocean Water) as defined by Gonfiantini (1978) using conventional delta ( $\delta$ ) notation in ‰. The precision of measurements ( $1\sigma$ ) was  $\pm 0.1\text{‰}$  for  $\delta^{18}\text{O}$  and  $\pm 1\text{‰}$  for  $\delta\text{D}$ . Stable isotopes of hydrogen and oxygen were analysed in the IAEA's Isotope Hydrology Laboratory in Vienna, and in the Institute of Geological and Nuclear Sciences, Lower Hutt, New Zealand.

### 3.5. Analysis of tritium

Tritium in water samples was analysed mass spectrometrically using the  $^3\text{He}$  in-growth method at the University of Miami, and by the electrolytical enrichment and liquid scintillation spectrometry in the IAEA's Isotope Hydrology Laboratory, and in the Institute of Geological and Nuclear Sciences. The results are expressed in tritium units (1 TU represents a ratio of 1 tritium ( $^3\text{H}$ ) atom to  $10^{18}$  protium ( $^1\text{H}$ ) atoms; it is equal to  $118 \text{ mBq L}^{-1}$  of water).

Analyses of IAEA reference materials and regular participation in intercomparison exercises helped to assure quality of analytical methods.

Table 3

Activity concentrations of Ra isotopes in seawater and in monitoring well (August 2002). The total relative uncertainties are below 10% (at  $1\sigma$  level)

Station	Sample type	Latitude	Longitude	Date	$^{223}\text{Ra}$ (mBq $\text{L}^{-1}$ )	$^{224}\text{Ra}$ (mBq $\text{L}^{-1}$ )	$^{226}\text{Ra}$ (mBq $\text{L}^{-1}$ )	$^{228}\text{Ra}$ (mBq $\text{L}^{-1}$ )	Salinity
A-1	Transect A	S23°32.052	W45°13.352	8	0.24	3.47	0.83	1.97	33.2
A-2	Transect A	S23°33.080	W45°12.002	7	0.12	1.63	0.80	1.85	33.1
A-3	Transect A	S23°33.963	W45°10.474	7	0.18	1.95	0.78	1.51	33.1
A-7	Transect A	S23°34.348	W45°04.678	6	0.04	0.74	1.18	1.67	33.3
A-8	Transect A	S23°34.625	W45°04.638	6	0.07	0.89	1.30	2.62	33.4
B-5	Transect B	S23°39.110	W45°04.341	6	0.05	0.62	1.47	2.87	33.7
B-7	Transect B	S23°36.220	W45°06.852	6	0.10	0.74	1.01	2.23	33.5
C-0	Transect C	S23°50.234	W45°11.132	8	0.09	0.24	1.65	2.42	33.2
C-1	Transect C	S23°46.511	W45°09.607	8	0.08	0.58	1.36	2.40	33.6
C-2	Transect C	S23°44.118	W45°11.208	8	0.08	0.61	0.89	2.53	33.6
C-3	Transect C	S23°39.390	W45°13.248	8	0.08	1.11	0.80	2.32	33.0
C-4	Transect C	S23°36.443	W45°16.992	8	0.13	1.40	0.95	2.15	32.9
T-1	Transect T	S23°35.422	W45°11.919	7	0.15	0.77	1.23	2.32	33.1
T-2	Transect T	S23°36.572	W45°13.008	7	0.09	0.88	1.68	3.02	33.2
T-3	Transect T	S23°38.489	W45°15.161	7	0.11	1.28	1.62	2.21	33.1
T-4	Transect T	S23°40.817	W45°17.834	7	0.15	1.45	0.96	2.45	33.1
T-5	Transect T	S23°43.324	W45°20.498	7	0.12	1.37	1.40	2.53	33.7
AB-1	Base	S23°29.952	W45°07.093	9	0.12	1.53	1.42	2.13	32.9
PM-4	Borehole well	S23°30.013	W45°07.095	9	1.41	73	1.60	8.88	33.1

Table 4  
Nutrients in seawater, seepage chamber and monitoring wells. The total relative uncertainties are below 1% (at 1 $\sigma$  level)

Station	Sample type	Latitude	Longitude	Date	Phosphate ( $\mu\text{mol L}^{-1}$ )	Silicate ( $\mu\text{mol L}^{-1}$ )	Nitrate ( $\mu\text{mol L}^{-1}$ )	Nitrite ( $\mu\text{mol L}^{-1}$ )	Salinity
<b>August 2002</b>									
A-1	Transect A	S23°32.052	W45°13.352	8	0.81	7.92	0.23	0.04	33.2
A-2	Transect A	S23°33.080	W45°12.002	7	0.74	7.25	0.25	0.08	33.1
A-3	Transect A	S23°33.963	W45°10.474	7	0.65	6.74	0.29	0.03	33.1
A-7	Transect A	S23°34.348	W45°04.678	6	0.85	6.09	0.30	0.12	33.3
A-8	Transect A	S23°34.625	W45°04.638	6	0.51	6.74	0.28	0.05	33.4
B-5	Transect B	S23°39.110	W45°04.341	6	0.69	6.89	0.33	0.16	33.7
B-7	Transect B	S23°36.220	W45°06.852	6	0.61	6.14	0.21	0.04	33.5
C-0	Transect C	S23°50.234	W45°11.132	8	0.55	6.95	0.34	0.22	33.2
C-1	Transect C	S23°46.511	W45°09.607	8	0.69	5.81	0.22	0.04	33.6
C-2	Transect C	S23°44.118	W45°11.208	8	0.55	8.12	0.25	0.24	33.6
C-3	Transect C	S23°39.390	W45°13.248	8	0.54	6.52	0.15	0.03	33.0
C-4	Transect C	S23°36.443	W45°16.992	8	0.47	5.02	0.16	0.07	32.9
T-1	Transect T	S23°35.422	W45°11.919	7	0.75	5.57	0.13	0.08	33.1
T-2	Transect T	S23°36.572	W45°13.008	7	0.61	7.04	0.12	0.13	33.2
T-3	Transect T	S23°38.489	W45°15.161	7	0.71	7.12	0.21	0.09	33.1
T-4	Transect T	S23°40.817	W45°17.834	7	0.62	6.65	0.11	0.11	33.1
T-5	Transect T	S23°43.324	W45°20.498	7	0.79	5.40	0.19	0.17	33.7
AB-1	Base	S23°29.952	W45°07.093	9	2.17	9.60	0.75	0.50	32.9
PM-4	Borehole well	S23°30.013	W45°07.095	9	3.47	9.12	0.73	0.29	33.1
<b>November 2003</b>									
PB-1	Picinquaba B.	23°21.930	44°51.288	17	0.33	7.0	0.09	0.07	33.77
PB-2	Picinquaba B.	23°21.755	44°51.258	17	0.30	4.74	0.25	0.14	33.93
PB-3	Picinquaba B.	23°21.655	44°51.458	17	0.38	5.48	0.27	0.10	33.95
PB-4	Picinquaba B.	23°21.583	44°51.871	17	0.38	5.9	0.91	0.03	33.94
PB-5	Picinquaba B.	23°21.580	44°56.451	17	0.34	6.04	0.36	0.14	33.97
PB-6	Picinquaba B.	23°22.860	44°57.406	17	0.44	7.51	0.13	0.03	33.63
PB-7	Picinquaba B.	23°23.405	44°58.100	17	0.44	5.78	0.10	0.03	33.93
PB-8	Picinquaba B.	23°24.132	44°59.773	17	0.34	6.46	0.10	0.03	33.68
PB-9	Picinquaba B.	23°21.426	44°51.026	20	0.28	3.45	0.10	<0.03	34.27
PB-10	Picinquaba B.	23°22.228	44°50.405	20	0.24	6.96	0.08	<0.03	33.78
PB-11	Picinquaba B.	23°21.662	44°51.446	20	0.12	10.6	0.3	0.14	33.18
PB-12	Picinquaba B.	23°21.594	44°51.913	20	0.34	8.46	0.06	0.07	33.17
FB-1	Flamengo B. transect	23°30.030	45°07.067	18	0.33	3.95	0.05	0.03	33.84
FB-2	Flamengo B. transect	23°29.938	45°06.998	18	0.34	4.98	0.07	0.03	33.77
FB-3	Flamengo B. transect	23°30.000	45°06.350	18	0.16	5.60	0.19	0.07	33.64
FB-4	Flamengo B. transect	23°29.295	45°06.343	18	0.18	6.00	0.27	0.07	33.59
FB-5	Flamengo B. transect	23°29.392	45°06.209	18	0.09	2.83	0.30	0.07	33.88
FB-6	Flamengo B. transect	23°29.734	45°05.035	18	0.21	3.04	0.30	0.14	33.99
FB-7	Flamengo B. transect	23°32.124	45°04.624	18	0.17	1.69	0.24	0.10	34.11
FB-12	Flamengo B. transect	23°32.234	45°03.853	18	0.18	1.90	0.05	0.03	34.19
FB-13	Flamengo B. transect	23°36.108	45°02.185	18	0.26	4.93	0.31	0.03	34.34
FB-14	Flamengo B. transect	23°38.064	45°00.015	18	0.17	6.55	0.48	0.07	34.31
FB-15	Flamengo B. transect	23°39.445	44°57.850	18	0.29	3.24	0.07	0.03	34.31
FB-16	Flamengo B. transect	23°40.627	44°55.595	18	0.10	2.84	0.35	0.07	34.27
V-8	Vitoria Isl. transect	23°40.582	44°55.600	19	0.09	6.40	0.64	0.14	34.32
V-9	Vitoria Isl. transect	23°44.930	45°00.040	19	0.14	3.87	0.05	0.03	34.23
V-10	Vitoria Isl. transect	23°45.258	45°01.476	19	0.18	2.40	0.10	0.03	34.21
V-11	Vitoria Isl. transect	23°42.895	45°03.213	19	0.12	4.53	0.21	0.07	34.34
V-12	Vitoria Isl. transect	23°40.383	45°04.942	19	0.30	5.17	0.19	0.07	34.02
V-13	Vitoria Isl. transect	23°38.685	45°06.825	19	0.30	3.92	0.10	0.03	34.15
V-14	Vitoria Isl. transect	23°36.354	45°08.384	19	0.09	4.51	0.43	0.07	34.14
V-15	Vitoria Isl. transect	23°34.238	45°10.368	19	0.18	14.0	0.10	0.03	33.76
V-16	Vitoria Isl. transect	23°32.594	45°12.741	19	0.18	7.66	0.28	0.03	33.73
SD-1	Seepage chamber	S23°30.003	W45°07.097	19	0.13	11.1	0.18	0.03	26.4
PM-4	Borehole well	S23°30.013	W45°07.095	19	0.69	3.21	1.73	1.19	32.9
PM-5	Borehole well	S23°30.018	W45°07.085	19	0.67	2.93	1.08	1.43	33.1
PM-7	Borehole well	S23°30.007	W45°07.093	19	0.55	3.07	1.34	0.54	31.0
PM-8	Borehole well	S23°30.012	W45°07.084	19	0.42	1.26	0.29	0.24	32.8

### 3.6. *In situ* analysis of $^{222}\text{Rn}$

$^{222}\text{Rn}$  is pure alpha-emitter decaying to  $^{218}\text{Po}$  ( $t_{1/2} = 3.05$  min), which then decays to  $^{214}\text{Pb}$  ( $t_{1/2} = 26.8$  min) and then to  $^{214}\text{Bi}$  (19.7 min), which has been used as the most suitable gamma-ray emitter for analysis of  $^{222}\text{Rn}$ , as it emits high intensity gamma-rays. The best visible photopeaks in the gamma-ray spectrum are due to  $^{214}\text{Pb}$  (352 keV) and  $^{214}\text{Bi}$  (609, 1120 and 1765 keV). Another radon isotope,  $^{220}\text{Rn}$ , is also pure alpha-emitter, which further decays to several short-lived daughter products including  $^{212}\text{Pb}$  ( $t_{1/2} = 10.64$  h, gamma-line 239 keV) and  $^{208}\text{Tl}$  ( $t_{1/2} = 183$  s, gamma-lines 583 and 2615 keV). As short-lived daughter products of both radon isotopes emit gamma-rays, *in situ* gamma-ray spectrometry is a suitable non-destructive technique for their analysis in seawater. It has the advantage of simultaneous analysis of other radionuclides as well, e.g.  $^{40}\text{K}$ , which is the dominant radionuclide in seawater ( $t_{1/2} = 1.96 \times 10^9$  y, gamma-line 1461 keV), but also  $^{228}\text{Ra}$ , via its daughter product  $^{228}\text{Ac}$  ( $t_{1/2} = 6.13$  h, gamma-line 911 keV),  $^{234}\text{Th}$ – $^{234}\text{Pa}$  ( $t_{1/2} = 24.1$  d and 71 s, gamma-lines 63, 93 and 1001 keV), and other radionuclides, especially when high resolution HPGe detectors, operating in seawater would be used (Osvath and Povinec, 2001).

The underwater gamma-ray spectrometer used in the 2003 expedition consisted of a 5 cm in diameter and 15 cm long NaI(Tl) scintillation crystal housed together with photomultiplier, high voltage power supply and signal processing electronics in a stainless steel tube 1 m long and 10 cm in diameter (Fig. 4). Additional sensors for monitoring of temperature, water depth and wave impacts are located in front of the NaI(Tl) detector. The detector unit was connected via a 70 m long, double armoured steel coaxial cable to a PC with processing electronics and multichannel analyzer located on a ship. The energy calibration of the gamma-spectrometer was carried out using  $^{137}\text{Cs}$  and  $^{60}\text{Co}$  radioactive sources. The energy resolution for 662 keV ( $^{137}\text{Cs}$ ) gamma-rays was 6.5%. The efficiency calibration was done using  $^{137}\text{Cs}$ ,  $^{40}\text{K}$

and  $^{226}\text{Ra}$  sources dispersed in a polyethylene tank filled with water. Background measurements were carried out with the detector immersed in the tank filled with fresh water. The detection limit for  $^{222}\text{Rn}$  measurements in seawater is  $0.05 \text{ kBq m}^{-3}$  and the reported total relative uncertainties (at  $1\sigma$  level) are below 20%. The corresponding  $^{214}\text{Bi}$  photopeaks used in spectra evaluations were either at 609, 1120 or 1765 keV, depending on background conditions during real measurements. The data acquisition system evaluates gamma-ray spectra every minute. Later the obtained spectra are usually integrated to 1 h intervals (depending on the type of measurement, e.g. a continuous long-term monitoring at one site or a spatial mapping), and the activity concentration of a selected radionuclide in fresh water or seawater is calculated. The system is fully automated and can operate without any surveillance.

A typical gamma-ray spectrum measured with the *in situ* gamma-spectrometer positioned at a depth of 2 m in Flamengo Bay is shown in Fig. 5. Several photopeaks are visible in the spectrum, notably the annihilation photopeak at 511 keV, the  $^{214}\text{Bi}$  photopeaks at 609, 1120 and 1765 keV, the  $^{228}\text{Ac}$  photopeak at 911 keV, the most dominant  $^{40}\text{K}$  photopeak in seawater at 1461 keV, and the  $^{208}\text{Tl}$  photopeak at 2615 keV.

Underwater gamma-ray measurements were carried out in several bays along the Ubatuba coast. We discuss here results obtained in Flamengo Bay, 15 m from the low tide shoreline, where continuous monitoring of  $^{222}\text{Rn}$  was carried out from 22 to 26 November, 2003. Further,  $^{222}\text{Rn}$  measurements in Flamengo and Pinguaba Bays, parallel with the coast, were carried out as well.

### 3.7. Analysis of radium isotopes

Acrylic fibre (Cia. Sudamericana do Brasil, 3.0 denier), treated with a hot solution of saturated  $\text{KMnO}_4$  for approximately 10 min, was used for pre-concentration of Ra isotopes from large volume (196 L) seawater samples. The prepared fibre was washed with purified water free of radium and was

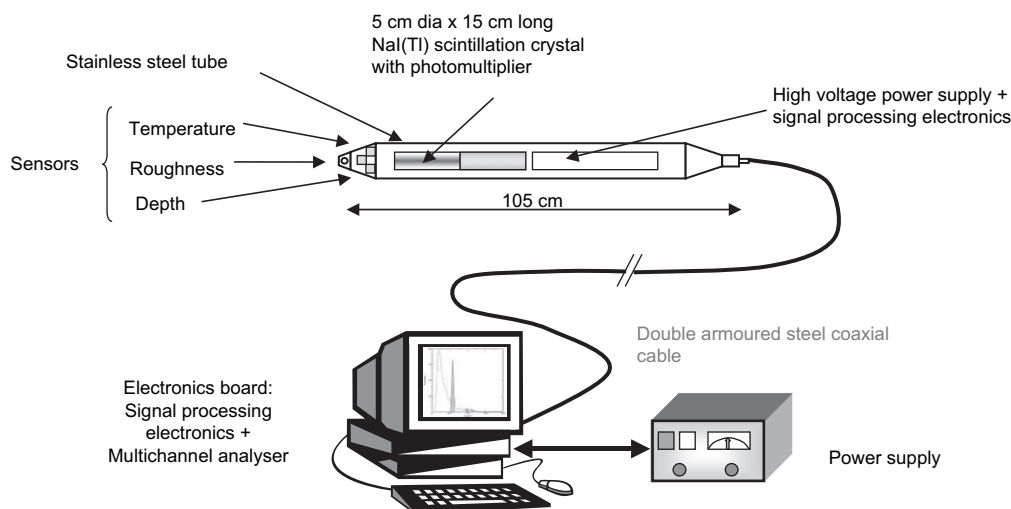


Fig. 4. Underwater gamma-spectrometer with electronics.

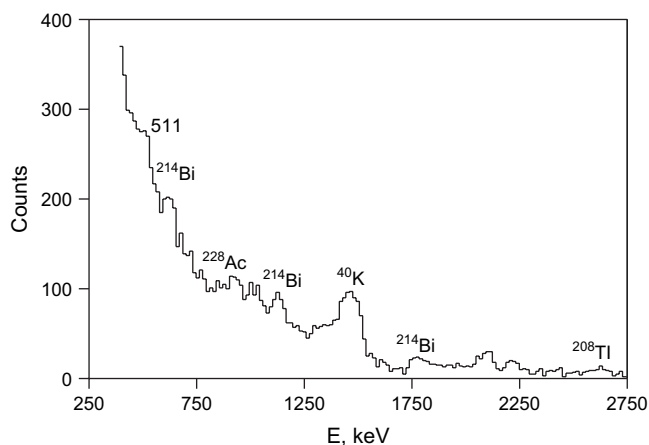


Fig. 5. *In situ* gamma-ray spectrum of seawater measured at Flamengo Bay. Several peaks are visible in the spectrum, notably the annihilation peak at 511 keV, the  $^{214}\text{Bi}$  peaks at 609, 1120 and 1765 keV, the  $^{228}\text{Ac}$  (a daughter product of  $^{228}\text{Ra}$  in the  $^{232}\text{Th}$  decay chain) peak at 911 keV, the most dominant  $^{40}\text{K}$  peak in seawater at 1461 keV, and the  $^{208}\text{Tl}$  (a daughter product of  $^{220}\text{Rn}$  in the  $^{232}\text{Th}$  chain) peak at 2615 keV.

kept in plastic bags for use during the sampling campaigns. Produced Mn fibres had sub-micrometre sized particles of  $\text{MnO}_2$  chemically bonded to the fibre. The  $\text{MnO}_2$  constitutes 8–10% by mass of the Mn fibre. Large volume seawater samples were pumped from  $\sim 2$  m below the surface into plastic drums on board the R/Vs Velliger II or Albacora. The sample volume was recorded and seawater was percolated through a column of manganese coated acrylic fibre to quantitatively remove radium from seawater (Moore, 1996).

At the Oceanographic Base onshore laboratory each Mn fibre sample was partially dried with a stream of air and placed in an air circulation system described by Moore and Arnold (1996). Helium was circulated over the Mn fibre to sweep  $^{219}\text{Rn}$  and  $^{220}\text{Rn}$  generated by  $^{224}\text{Ra}$  and  $^{223}\text{Ra}$  decays in a 1.1 L scintillation cell. The alpha particles from the decay of radon and its daughters were recorded by a photomultiplier tube (PMT) attached to the scintillation cell. Signals from the PMT were routed to a delayed coincidence counter system adapted for Ra measurements, which utilizes the difference in decay constants of the short-lived Po daughters of  $^{219}\text{Rn}$  and  $^{220}\text{Rn}$  to identify alpha particles derived from  $^{223}\text{Ra}$  and  $^{224}\text{Ra}$  captured on the Mn fibre (Moore and Arnold, 1996). The relative uncertainty of the short-lived Ra isotope measurements was better than 10%. After completing the  $^{224}\text{Ra}$  and  $^{223}\text{Ra}$  measurements, the Mn fibre samples were aged for 5 weeks to allow the excess  $^{224}\text{Ra}$  to equilibrate with  $^{228}\text{Th}$ , also adsorbed on the Mn fibre. The samples were then measured again to determine the  $^{228}\text{Th}$  activity, and to correct the  $^{224}\text{Ra}$  activity to its unsupported activity.

Following these analyses, the Mn fibre was leached in a beaker with 200 mL of HCl under controlled heating, to quantitatively remove the longer-lived Ra isotopes. For the radiochemical separation of  $^{226}\text{Ra}$  and  $^{228}\text{Ra}$ , carriers of stable barium (20 mg) and lead (20 mg) were added to the water sample in the presence of 5 mL of 1 M citric acid and 5 mL of 40% hydroxylamine hydrochloride solutions. The radium

was co-precipitated as  $\text{BaPb(Ra)SO}_4$  by adding 50 mL of 3 M  $\text{H}_2\text{SO}_4$ . The precipitate was dissolved with alkaline EDTA. When the pH is adjusted to 4.5 with glacial acetic acid,  $\text{Ba(Ra)SO}_4$  is re-precipitated, while interfering elements remain in the solution. The  $\text{Ba(Ra)SO}_4$  precipitate was transferred to a 2 mL polypropylene tube and sealed to avoid the escape of  $^{222}\text{Rn}$ .  $^{226}\text{Ra}$  and  $^{228}\text{Ra}$  were measured by gamma-spectrometry of a  $\text{Ba(Ra)SO}_4$  precipitate in a HPGe germanium detector (n-type detector from Eurisy Measures, relative efficiency 15%, resolution 1.90 keV at 1332 keV of  $^{60}\text{Co}$ ), after 21 days from the precipitation. The  $^{226}\text{Ra}$  activities were determined (after  $>20$  days sample storage) by taking the mean activity of three separate photopeaks of its daughter nuclides:  $^{214}\text{Pb}$  at 295.2 keV and 351.9 keV, and  $^{214}\text{Bi}$  at 609.3 keV. The  $^{228}\text{Ra}$  content of the samples was determined from the 911 keV and 968 keV photopeaks of  $^{228}\text{Ac}$ . All the activity results were decay corrected to the sampling date. Uncertainties are reported as the combined standard uncertainty (at  $1\sigma$  level). In order to determine any bias, the method validation procedure was carried out via the analysis of matrix matched reference materials (multi-radionuclide prepared standards and traceable reference materials), with identical sample counting geometry and detector configuration. The uncertainty components were combined following the root-sum-of-squares rule to give the combined standard uncertainty for each nuclide. The expanded uncertainty was obtained by the error propagation formula, considering all variables to be independent. The systematic uncertainty component consisted of the calibration source uncertainty (less than 1.5%) and calibration curve fitting uncertainty (less than 1%). These measurements were carried out at Laboratório de Radiometria Ambiental, Instituto de Pesquisas Energeticas e Nucleares (IPEN), São Paulo.

### 3.8. Analysis of nutrients

The analytical procedures included a vanadium method for nitrate–nitrite, a phenate method for ammonia, and an ascorbic acid method for phosphate. The measurements were performed at Laboratório de Nutrientes, Micronutrientes e Traços do Mar, Instituto Oceanográfico da Universidade de São Paulo (Braga and Muller, 1998). The total relative uncertainties (not shown in the tables) were below 1% (at  $1\sigma$  level). Reference samples were analysed simultaneously.

## 4. Results

### 4.1. Salinity

Measurement of salinity is the simplest way to recognise SGD in coastal waters, although it may not give full information, as SGD may be represented by a mixture of groundwater and re-circulated seawater. The geographical locations of the sampling sites surveyed in August 2002 and November 2003, as well as the isotopic composition (deuterium,  $^{18}\text{O}$ ,  $^3\text{H}$ ), salinity and temperature of samples collected on the continent (rain and river water, groundwater springs and in-land

wells, and monitoring borehole wells) and at the sea (seawater, seepage chambers, piezometers and monitoring borehole wells) are presented in Table 1.

During the mission in August 2002 (winter), the water column was well stratified with a strong thermocline at middle depths (around 10 m). On the other hand, salinity profiles measured in Flamengo and Picinguaba Bays showed that during November 2003 (summer) the water column was well mixed. Continuous monitoring of salinity in Flamengo Bay during 22–26 November showed variations between 33.9 and 35.3, depending on the tide. Generally, the salinity record follows the tide record; however, on 26 November a delay in the salinity record was observed. Salinity along the Ubatuba coast (Tables 1, 2 and 4) varied from 32.0 to 34.8, showing lower values than in south-western Atlantic waters ( $\sim 35$ ). The variability in salinity values observed both at the Flamengo and Picinguaba Bays indicated possible SGD sources in the area.

Salinity measurements in monitoring wells and piezometers, as well as in water collected in seepage bags (Fig. 3), showed temporal variations slightly depending on the tide level. The observed salinity levels in monitoring wells ranged from typical fresh water values ( $\sim 0.0$  for PM-1 and PM-3) up to 34.0 for PM-4 which has been influenced by seawater. Salinity in samples collected in piezometer tubes at depths of  $\sim 10$  cm below the sediment surface varied between 31.9 and 33.6, while at depths of  $\sim 100$  cm salinities were 1.6 and 33 for MS-5/4 and MS-4/5, respectively, showing different groundwater influence at 6.5 m (MS-5) and 35 m (MS-4) distance from the shoreline. Salinity of analysed water samples from seepage chambers varied between 25.5 and 26.2 (the lowest value (20) was measured in the seepage chamber SD-1E, located on the shoreline, Bokuniewicz et al., 2008).

#### 4.2. Stable isotopes and tritium in fresh water samples

The isotopic composition of rain samples collected in August 2002 and November 2003 showed typical values expected for the Southern Hemisphere. The hydrogen ( $\delta D$ ) and the oxygen ( $\delta^{18}O$ ) isotope compositions varied between  $-20.0$  and  $-17.5\text{‰}$ , and between  $-3.7$  and  $-3.5\text{‰}$ , respectively. Tritium levels measured in rain water were around 2.5 TU. The isotope composition of river water sampled at Fazenda Beach (Picinguaba Bay) in 2003 varied from  $-15.6$  to  $-9.3\text{‰}$  for  $\delta D$ , and between  $-3.61$  and  $-2.92\text{‰}$  for  $\delta^{18}O$ , showing values which were close to the rain values. Tritium levels in river water were around 2.5 TU, within uncertainties the same as for precipitation. Groundwater springs and wells had  $\delta D$  in the range of  $-18.3$  to  $-11.2\text{‰}$ , while the  $\delta^{18}O$  values were between  $-3.9$  and  $-3.17\text{‰}$ . Tritium levels ranged from 2.1 to 2.7 TU. The groundwater spring found at the Oceanographic Base showed similar stable isotope and tritium levels as the groundwater spring found on the road about 10 km from the Base (used by local population as a source of drinking mineral water), and is one of the groundwater end-member candidates. Samples collected in 2002 and 2003 showed a similar  $\delta D$ ,  $\delta^{18}O$  and  $^3H$  composition.

#### 4.3. Stable isotopes, $^3H$ , $^{222}Rn$ and trace elements in mixed groundwater–seawater samples

Isotope results (Table 1) for water samples collected in monitoring borehole wells (Fig. 3) were between groundwater and seawater samples. Stable isotopes varied for  $\delta D$  from  $-14.7$  to  $3.9\text{‰}$  and from  $-3.20$  to  $0.49\text{‰}$  for  $\delta^{18}O$ . Wells PM-1 and PM-6 represented fresh water, while other wells were showing either a mixture of fresh–seawater or seawater only (PM-4, 5, 7 and 8). This has also been confirmed by elemental analysis (Table 2) as PM-1 well located in the garden, had fresh water during low tide (Cl content below  $0.001 \text{ mg g}^{-1}$ ), and during high tide there was a small admixture of seawater (Cl content  $\sim 0.07 \text{ mg g}^{-1}$ ). Similarly, wells PM-3 and PM-6 showed the presence of fresh water, while other wells showed a typical seawater elemental composition (Cl content  $\sim 19 \text{ mg g}^{-1}$ ).

$\delta D$  values (Table 1) in porewater sampled from piezometer multisampler MS-5 (Fig. 3) varied from  $-13.1$  to  $0.06\text{‰}$  and  $\delta^{18}O$  from  $-0.32$  to  $-0.15\text{‰}$ , while MS-4 showed  $\delta D$  values between  $0.05$  and  $3.1\text{‰}$ , and  $\delta^{18}O$  between  $0.14$  and  $0.35\text{‰}$ . While the site MS-5 was influenced by groundwater ( $^3H$ :  $1.9$ – $2.2$  TU and Cl:  $0.15$ – $2.5 \text{ mg g}^{-1}$ , except for the surface layer which showed the presence of seawater), the site MS-4 situated 35 m offshore showed tritium ( $1.0$ – $1.4$  TU) and chlorine ( $\sim 19 \text{ mg g}^{-1}$ ) levels typical for seawater.

The isotopic composition (Table 1) of water samples collected in seepage chambers (Fig. 3) was between seawater and groundwater as well.  $\delta D$  results were between  $0.4$  and  $0.6\text{‰}$ , and  $\delta^{18}O$  between  $-0.07$  and  $0.0\text{‰}$ , documenting that re-circulated seawater with a small admixture of groundwater has been playing a dominant role in the seepage. Tritium concentration ( $2.1$  TU) measured in the seepage chamber SD-1E was similar to the one measured in the piezometer multisampler MS-5, situated only 6.5 m from the shoreline where SD-1E was located. Time series of water samples collected in the seepage chamber SD-1E showed Cl content of  $\sim 15 \text{ mg g}^{-1}$ , confirming a presence of freshwater, the concentration of which did not change with tide. Seepage chambers SD-2 and SD-5 were even more influenced by seawater (as expected from samples collected in piezometer tubes), having  $\delta D$  values between  $0.0$  and  $1.7\text{‰}$ , and  $\delta^{18}O$  between  $-0.12$  and  $0.15\text{‰}$ .

Stable isotopes in seawater samples (Table 1) are characterised by significant variability and enrichment of  $\delta^{18}O$ , which has been very different from groundwater samples. Seawater samples had mostly positive values, from  $1.0$  to  $4.6\text{‰}$  for  $\delta D$ , and from  $-0.02$  to  $0.53\text{‰}$  for  $\delta^{18}O$ . Tritium levels in visited bays varied between  $0.9$  and  $2.7$  TU. They did not show any correlation with sampled water depth, which varied between 2 and 40 m. Elemental data presented in Table 2 show that the seawater samples are rich in chlorine ( $\sim 19 \text{ mg g}^{-1}$ ), sulphur ( $\sim 0.7 \text{ mg g}^{-1}$ ), potassium ( $\sim 0.4 \text{ mg g}^{-1}$ ), calcium ( $\sim 0.4 \text{ mg g}^{-1}$ ) and bromine ( $\sim 0.08 \text{ mg g}^{-1}$ ). Lower concentrations were observed for strontium ( $\sim 0.008 \text{ mg g}^{-1}$ ) and barium ( $\sim 0.006 \text{ mg g}^{-1}$ ). On the contrary, the groundwater samples (sampled, e.g. on the Flamengo Beach) are low in those elements where seawater was rich, but

comparable in others. The same observations were made for spring and river water sampled at Enseada and Perequê-Mirin beaches.

Surface distribution of  $^{222}\text{Rn}$  in seawater was investigated in Flamengo and Picinguaba Bays. In Flamengo Bay, the  $^{222}\text{Rn}$  activity concentrations observed at five stations varied between 50 and 200  $\text{Bq m}^{-3}$ , the highest values were found close to the Oceanographic Base, and at Perequê-Mirin Beach. Four stations visited in Picinguaba Bay showed  $^{222}\text{Rn}$  activity concentrations between 50 and 140  $\text{Bq m}^{-3}$ .

Time series of  $^{222}\text{Rn}$  activity concentration in seawater, salinity and tide were recorded from 22 to 26 November 2003, in Flamengo Bay, 15 m offshore the Oceanographic Base, where largest SGD fluxes were observed by the seepage meters group (Bokuniewicz et al., 2008; Taniguchi et al., 2008). The  $^{222}\text{Rn}$  activity concentrations varied between 1.1 and 5.2  $\text{kBq m}^{-3}$ , while the tide level varied between 4.4 and 5.6 m.

#### 4.4. Radium isotopes and nutrients

$^{223}\text{Ra}$ ,  $^{224}\text{Ra}$ ,  $^{226}\text{Ra}$  and  $^{228}\text{Ra}$  data collected during the August 2002 expedition are presented in Table 3. Large variations in Ra isotopic composition of surface seawater were observed.  $^{223}\text{Ra}$  activity concentrations varied from 0.04 to 0.2  $\text{Bq m}^{-3}$ ,  $^{224}\text{Ra}$  from 0.2 to 3.5  $\text{Bq m}^{-3}$ ,  $^{226}\text{Ra}$  from 0.8 to 1.7  $\text{Bq m}^{-3}$  and  $^{228}\text{Ra}$  from 1.5 to 3  $\text{Bq m}^{-3}$ . Due to elevated concentrations of  $^{232}\text{Th}$  in the region, it was possible to measure for the first time  $^{228}\text{Ra}$  concentrations in seawater using the *in situ* gamma-spectrometer (via its daughter gamma-ray emitter  $^{228}\text{Ac}$ ).  $^{228}\text{Ra}$  activity concentrations measured in Flamengo and Picinguaba Bays varied between 1.6 and 3.3  $\text{Bq m}^{-3}$  and they were following the  $^{222}\text{Rn}$  concentrations measured at the same stations. Much higher Ra concentrations were observed in August 2002 in monitoring borehole well PM-04:

1.4  $\text{Bq m}^{-3}$ , 73  $\text{Bq m}^{-3}$ , 1.6  $\text{Bq m}^{-3}$  and 8.9  $\text{Bq m}^{-3}$  for  $^{223}\text{Ra}$ ,  $^{224}\text{Ra}$ ,  $^{226}\text{Ra}$  and  $^{228}\text{Ra}$ , respectively, documenting that this well was influenced by groundwater.

Nutrient data are summarised in Table 4. Silicates, phosphates, nitrates and nitrites were analysed in all collected samples. The results show a wide range of values, the highest for silicates (from 2 to 14  $\mu\text{mol L}^{-1}$ ), phosphates (from 0.1 to 0.9  $\mu\text{mol L}^{-1}$ ) and nitrates (from 0.05 to 0.9  $\mu\text{mol L}^{-1}$ ). A nutrient content variability with distance/salinity offshore has been found.

## 5. Discussion

### 5.1. Isotope geochemistry

The local meteoric water line (LMWL) for the São Paulo region was constructed on the basis of the IAEA's GNIP (Global Network of Isotopes in Precipitation) database (<http://www.iaea.org>). The calculated LMWL can be represented by the equation

$$\delta\text{D} = 8.1\delta^{18}\text{O} + 5.2 \quad (1)$$

which can be compared with the global meteoric water line (GMWL) defined after Craig (1961) as

$$\delta\text{D} = 8\delta^{18}\text{O} + 10 \quad (2)$$

In the  $\delta\text{D}$  versus  $\delta^{18}\text{O}$  diagram groundwater springs, rain, river and some of the monitoring wells data are grouped above the GMWL, while the seawater data are below this line (Fig. 6). The LMWL calculated for the São Paulo inland region does not fit well with the data set, probably due to an influence of the sea on the isotopic composition of rains. The regression line through the groundwater–seawater data (correlation coefficient  $r^2 = 0.97$ ,  $P < 0.0001$ ) shows a lower slope than that for

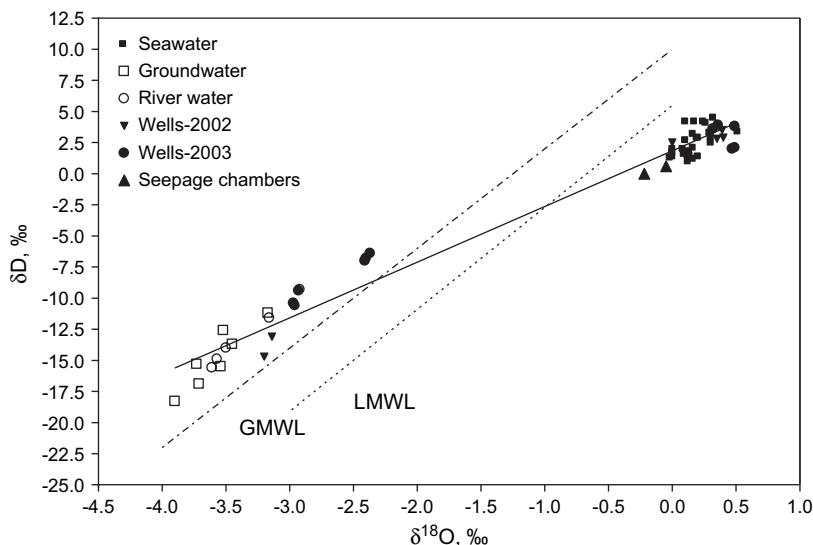


Fig. 6.  $\delta\text{D}$  vs.  $\delta^{18}\text{O}$  plot for groundwater, seawater and their mixtures (water in monitoring wells and in seepage chambers). GMWL, global meteoric water line (constructed after Craig, 1961); LMWL, local meteoric water line (constructed using the IAEA's GNIP (Global Network of Isotopes in Precipitation) data). Notice the differences between the GMWL (LMWL) and the regression line for the groundwater–seawater data (correlation coefficient  $r^2 = 0.97$ ,  $P < 0.0001$ ), which could be due to an influence of seawater–atmospheric water vapor interactions.

the GMWL and LMWL. This could be due to seawater–atmospheric water vapour interactions and non-equilibrium isotopic fractionation of groundwater after its infiltration and underground circulation in this issue.

The groundwater is depleted in  $^{18}\text{O}$  with respect to the VSMOW, while the seawater samples are highly enriched in  $^{18}\text{O}$ . The diagram in Fig. 6 confirms that groundwater samples are well separated from seawater samples. Therefore in the majority of cases there has not been significant mixing of groundwater with seawater at the visited sites. The water samples from monitoring wells and seepage chambers are situated between the both main groups of samples, representing mixtures of groundwater and seawater. The variability in D and  $^{18}\text{O}$  enrichment may be caused by different seawater contributions to the collected samples as re-circulated seawater is playing a dominant role in coastal groundwater–seawater interactions. The original composition of the groundwater component entering the sea floor may therefore be different. The  $\delta^{18}\text{O}$  vs. salinity plot (Fig. 7) is also showing good separation of groundwater and seawater groups ( $r^2 = 0.99$ ,  $P < 0.0001$ ), confirming that  $\delta^{18}\text{O}$  values are well representing the salinity. The tritium data presented in the same figure show a weak negative correlation on salinity ( $r^2 = 0.50$ ,  $P = 0.0005$ ).

The isotope composition ( $\delta\text{D}$ ,  $\delta^{18}\text{O}$  and  $^3\text{H}$ ) of submarine waters is characterised by significant variability and heavy isotope enrichment, with  $\delta\text{D}$  values between  $-15$  and  $4.5\text{‰}$ ,  $\delta^{18}\text{O}$  between  $-3.20$  and  $0.5\text{‰}$ , and  $^3\text{H}$  between 1.0 and 2.2 TU. The groundwater end-member can be represented by groundwater springs observed at the Oceanographic Base (GS-1), on the road (GS-2), and at the Corsario site (GW-1), which showed similar isotopic compositions ( $\delta\text{D}$  values between  $-18$  and  $-12\text{‰}$ ,  $\delta^{18}\text{O}$  between  $-3.9$  and  $-3.2\text{‰}$ , and  $^3\text{H}$  between 2.0 and 2.7 TU). On the other hand, the seawater end-member may be represented by open sea samples collected between the coast and Vitoria Island with  $\delta\text{D}$  and

$\delta^{18}\text{O}$  values around 3.0 and  $0.5\text{‰}$ , respectively, and  $^3\text{H}$  around 1.2 TU. Using a simple two end-members mixing model, we can calculate that the contribution of groundwater in submarine waters may vary from a few % to 17%, depending on the location and the tide level. The SGD may be therefore mostly represented by coastal groundwater and re-circulated seawater with small proportions of groundwater in the mixture. Offshore Ubatuba we did not find a single strong SGD source like, e.g. in the Donnalucata region, south-eastern Sicily (Povinec et al., 2006b).

## 5.2. Variations of radon concentration in seawater

An inverse relationship between the observed  $^{222}\text{Rn}$  activity concentration of surface seawater and salinity is demonstrated in Fig. 8 for Flamengo and Pinguaba Bays ( $r^2 = 0.93$ ,  $P = 0.035$  and  $r^2 = 0.92$ ,  $P = 0.039$ ), respectively. The negative correlation indicates that waters with lower salinity have higher  $^{222}\text{Rn}$  concentrations due to an admixture of groundwater in the system. The  $^{222}\text{Rn}$  activity concentrations at Flamengo Bay were up to 100 times higher than in Pinguaba Bay (at similar salinities), that would suggest different sources of groundwater in the bays. Generally, there was a rapid loss of  $^{222}\text{Rn}$  from groundwater to saline waters, as its levels in monitoring borehole wells in Flamengo Bay were much higher (from 4 to 25  $\text{kBq m}^{-3}$  for PM-6 and PM-1, respectively). Elevated  $^{222}\text{Rn}$  activity concentrations were also observed by Cable and Martin (2008) in multi-level piezometers (e.g. for MS-5 from 4 to 16  $\text{kBq m}^{-3}$ , depending on the porewater sampling depth).

$^{222}\text{Rn}$  time series in Flamengo Bay (Fig. 9) showed a weak negative correlation of its activity concentration with tidal stage, when during decreasing sea level  $^{222}\text{Rn}$  concentration was slightly increasing, and vice versa, during high tides  $^{222}\text{Rn}$  concentration was decreasing. This may be caused by

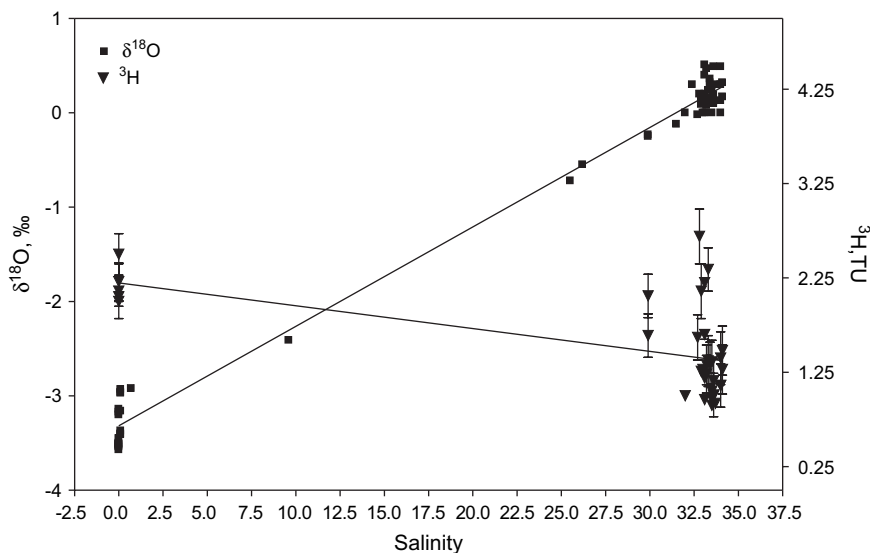


Fig. 7. Tritium and  $\delta^{18}\text{O}$  vs. salinity plot for collected groundwater and seawater samples and their mixtures.  $\delta^{18}\text{O}$  is well representing salinity (correlation coefficient  $r^2 = 0.99$ ,  $P < 0.0001$ ). The tritium vs. salinity plot also shows good separation of groundwater and seawater groups of samples, however, with a weak negative correlation ( $r^2 = 0.50$ ,  $P = 0.0005$ ).

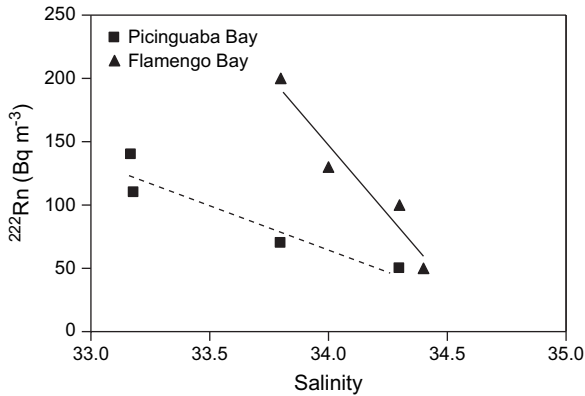


Fig. 8. An inverse relationship between the observed <sup>222</sup>Rn activity concentration of seawater and salinity for Flamengo and Pinguaba Bays ( $r^2 = 0.93$ ,  $P = 0.035$  and  $r^2 = 0.92$ ,  $P = 0.039$ ), respectively. <sup>222</sup>Rn activity concentrations in surface seawater at Flamengo Bay were up to 100 times higher than in Pinguaba Bay (at similar salinities), which would indicate different sources of groundwater in the bays. Generally, there was a rapid loss of <sup>222</sup>Rn from groundwater to saline waters, as its levels in monitoring borehole wells in Flamengo Bay were much higher (from 4 to 25 kBq m<sup>-3</sup>).

sea level changes as tide effects induce variations of hydraulic gradients, which increase <sup>222</sup>Rn concentration during lower sea level, and vice versa, during high tides where the <sup>222</sup>Rn activity concentration is smaller (Povinec et al., 2006b). A few hours shift between the tide minimum and <sup>222</sup>Rn activity concentration maximum (and vice versa) was observed. However, this usual inverse relationship between the <sup>222</sup>Rn activity concentration in seawater and tide/salinity was not observed during 22 November, despite large variations in water level and high salinities. The observed salinities (from 34.7 to 35.3) were much higher than during 25 and 26 November (showing,

however, small changes with tide during this time), which would indicate that the Bay on 22 November was predominantly occupied by waters from the open sea (SACW), having higher salinity (35–36) and lower <sup>222</sup>Rn concentration. The expected inverse relationship between the <sup>222</sup>Rn activity concentration in seawater and tide/salinity was seen from 23 to 25 November, when the Bay was again under the influence of groundwater discharge.

The inverse relationship between the <sup>222</sup>Rn activity concentration and tide in Flamengo Bay was also reported by Burnett et al. (2008), who analysed <sup>222</sup>Rn in seawater by alpha-ray spectrometry of its daughter products. The observed temporal changes in <sup>222</sup>Rn concentration between 16 and 20 November 2003 were from 20 to 100 Bq m<sup>-3</sup>. Fifty times higher <sup>222</sup>Rn concentrations presented in Fig. 9 may be due to a position of the monitoring site, which was closer to the shoreline (15 m vs. 200 m in Burnett et al., 2008), where large SGD fluxes were observed by seepage meter groups (Bokuniewicz et al., 2008; Taniguchi et al., 2008), and the piezometer group (Cable and Martin, 2008) reported high <sup>222</sup>Rn concentrations in porewater (up to 15 kBq m<sup>-3</sup>). The <sup>222</sup>Rn concentrations measured with underwater gamma-spectrometer at other sites of Flamengo Bay (Fig. 8) were comparable with the results obtained by Burnett et al. (2008).

When comparing the obtained results with similar measurements recently carried out offshore south-eastern Sicily (Povinec et al., 2006b) we observe that at the Sicilian site the <sup>222</sup>Rn concentrations were strongly dependent on the tide, although only small changes in tide were observed (10 cm in Sicily vs. 120 cm in Brazil). <sup>222</sup>Rn concentrations in seawater at Sicilian and Brazilian sites were very similar, between 2 and 5 kBq m<sup>-3</sup>, and 1 and 5 kBq m<sup>-3</sup>, respectively. In contrast

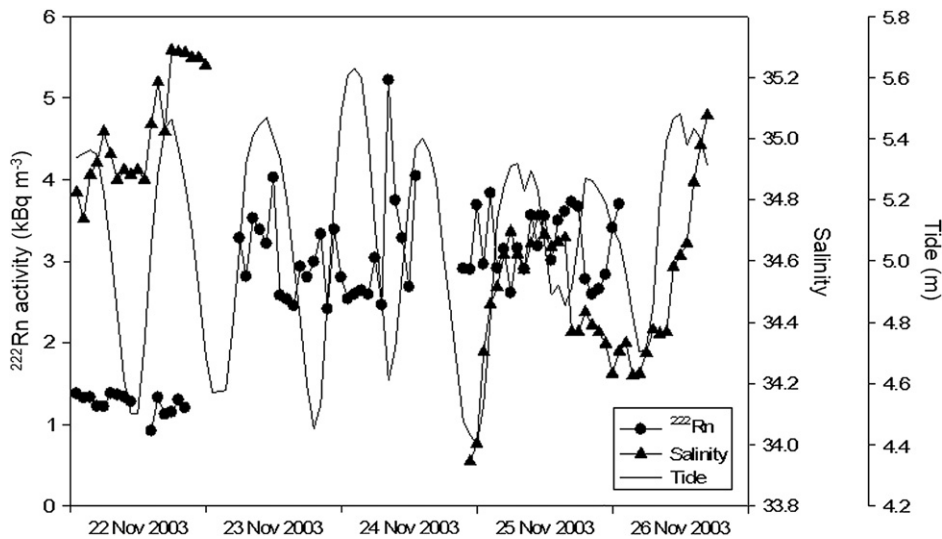


Fig. 9. Time-series <sup>222</sup>Rn measurements together with salinity and tide in Flamengo Bay at a fixed location 15 m from the low tide shoreline. A negative correlation of <sup>222</sup>Rn activity concentration with tidal stage was observed, when during decreasing sea level, <sup>222</sup>Rn concentration was increasing and vice versa, during high tides <sup>222</sup>Rn concentration was decreasing. A few hours shift between the tide minimum and <sup>222</sup>Rn activity concentration maximum (and vice versa) can be seen. However, this usual inverse relationship between the <sup>222</sup>Rn activity concentration in seawater and tide/salinity was not observed during 22 November, despite large variations in water level and higher salinities. This would indicate that the Bay on 22 November was predominantly occupied by seawater from the open sea (SACW) having higher salinity and lower <sup>222</sup>Rn concentration. The expected inverse relationship between the <sup>222</sup>Rn activity concentration in seawater and tide/salinity was seen from 23 to 25 November, when the Bay was again under the influence of groundwater discharge.

to the Sicilian sites, which represent a typical karstic region with low concentrations of U and Th, the Brazilian sites are characterised by granite rocks where the concentrations of  $^{238}\text{U}$  and  $^{232}\text{Th}$  in collected rock and sediment samples were higher (between 0.3 and 3 ppm for U, and 0.3 and 15 ppm for Th). Therefore, higher  $^{222}\text{Rn}$  activity concentrations in groundwater and seawater along the Ubatuba coast would be expected. The observed  $^{222}\text{Rn}$  levels in Flamengo and Picin-guaba Bays indicate (also supported by the stable isotope data) that the admixture of fresh water in submarine waters is much lower than in Sicily, where levels up to 50% were observed (Povinec et al., 2006b). SGD in the Ubatuba region is therefore mostly represented by re-circulated seawater, having a lower  $^{222}\text{Rn}$  concentration.

### 5.3. Offshore distribution of radium isotopes and nutrients

Very good indicators of groundwater inputs in coastal seawater are short-lived  $^{223}\text{Ra}$  and  $^{224}\text{Ra}$ , as they are easily flushed from sediments and rapidly regenerated from their thorium parents on a time scale of days. Such a continuous supply of  $^{223}\text{Ra}$  and  $^{224}\text{Ra}$  is not accompanied by large additions of long-lived

$^{226}\text{Ra}$ , which is regenerated only slowly. Fig. 10 shows the distribution of  $\ln^{223}\text{Ra}$  and  $\ln^{224}\text{Ra}$  in excess with distance offshore. Theoretically, in the semi-logarithmic scale their concentrations should decrease linearly with distance, which has been observed for all three transects. For long lived  $^{226}\text{Ra}$ , we would expect  $\ln^{226}\text{Ra}$  to be constant with offshore distance. An even better approximation could be the activity ratio, i.e.  $\ln[^{224}\text{Ra}/^{223}\text{Ra}]$ , as this is primarily dependent on source conditions. The observed increase of this activity ratio for the transect C at about 15 km from the coast, also presented in Fig. 10, may indicate either an influence of SACW upwelling or offshore SGD.

The nutrient levels in a coastal area are influenced both by transport of coastal waters in bays and by groundwater discharge in the region (Paytan et al., 2006; Boehm et al., 2006). Except for silicates, higher nutrient levels were observed in monitoring wells (Table 4) which may be due to an infiltration of groundwater contaminated by domestic sewage. Generally the nutrient levels observed in wells and in seawater were higher in 2002 than in 2003. When comparing the nutrients data offshore (Fig. 11, especially silicates) with  $\ln[^{224}\text{Ra}/^{223}\text{Ra}]$  activity ratios (Fig. 10) we see similar trends in transect C, where both data sets show maxima between 15 and 20 km. This signal may be again due to the presence of SACW over the shelf.

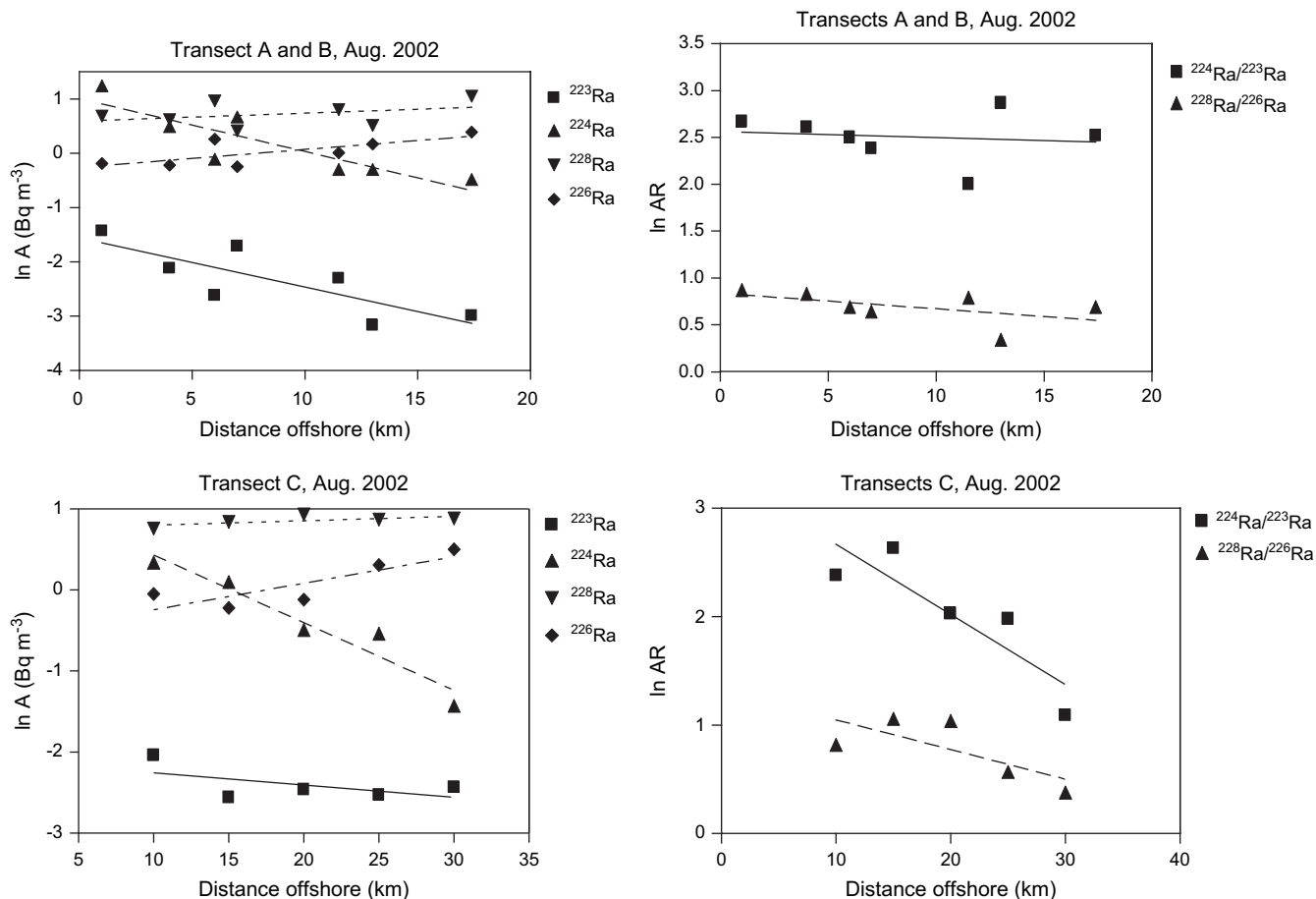


Fig. 10. The distribution of  $\ln^{223}\text{Ra}$  and  $\ln^{224}\text{Ra}$  in excess with distance offshore. Theoretically, in the semi-logarithmic scale their concentrations should decrease linearly with distance, which is a case for all three transects. For long-lived  $^{226}\text{Ra}$  isotope  $\ln^{226}\text{Ra}$  is expected to be constant with distance. An even better approximation could be the activity ratios, i.e.  $\ln[^{224}\text{Ra}/^{223}\text{Ra}]$ , as this is primarily dependent on source conditions. The observed increase of this activity ratio at about 15 km from the coast (transect C) may indicate either an influence of SACW upwelling or an offshore SGD.

The scattered nutrient data presented in Fig. 11, even an increase of nutrient contents with offshore distance would indicate that an important source of nutrients in the area would be a transport offshore water masses to the bays. In some places, the sea was visibly much more polluted far from the coast than close to the shoreline, due to water and pollutant transport by local currents. Observed nitrate and phosphate concentrations are typical for the oligomesotrophic region found at the Ubatuba marine ecosystem (Braga and Muller, 1998).

The concentration of nutrients vs. salinity plot (Fig. 12) for samples collected in 2003 is showing similar scattered nutrient data as in 2002. In the complex coastal region with many small bays and islands, the area has been influenced by local currents and by groundwater–seawater mixing. This has also been confirmed by a short residence time of 1–2 weeks for waters within 25 km of the shore (Moore and de Oliveira, 2008).

#### 5.4. Submarine groundwater discharge estimates

We are developing a general model of groundwater–seawater interactions in coastal areas, which is based on oceanographic parameters (tide, waves, salinity, temperature, seepage rates) as well as on chemical tracers (stable isotopes, tritium, radium quartet, radon, trace elements and nutrients).

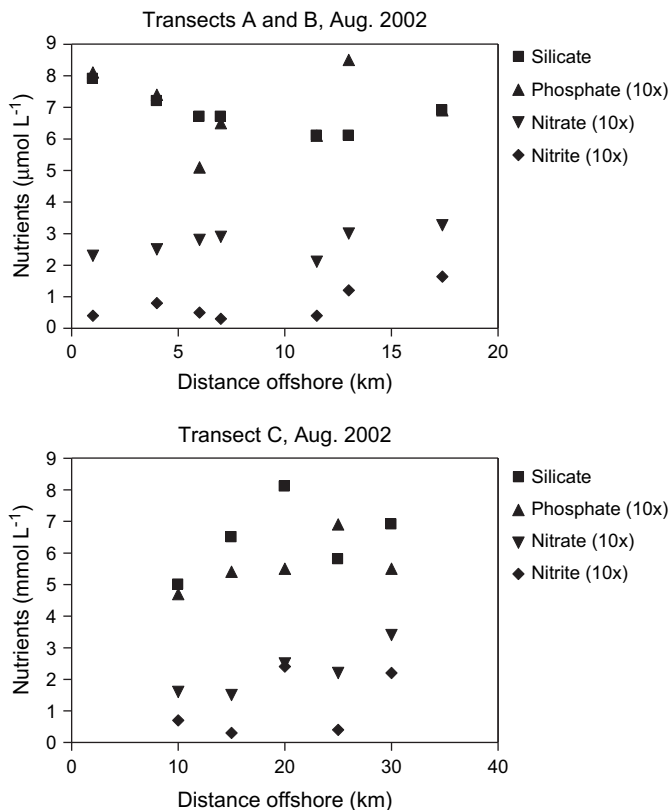


Fig. 11. Concentrations of nutrients vs. offshore distance (2002). The scattered nutrient data and even an increase of nutrient contents with offshore distance would indicate that an important source of nutrients in the area would be a transport offshore water masses to the bays. The higher nutrient contents observed at 20 km offshore at transect C may be due to the presence of SACW over the shelf.

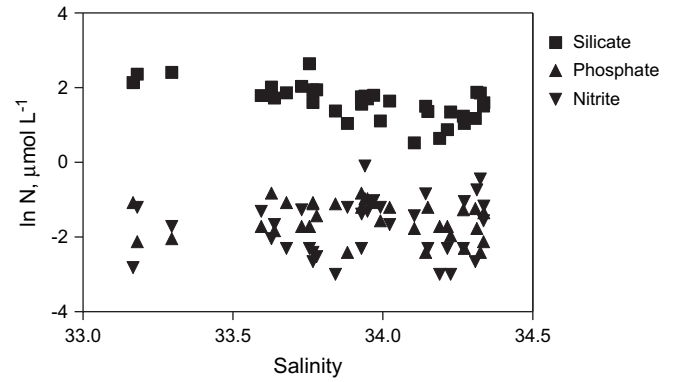


Fig. 12. The distribution of  $\ln N$  (concentration of nutrients) as a function of salinity for samples collected in 2003. The scattered nutrient data show a similar trend as in 2002, confirming that the coastal area was under an influence of local currents and SGD.

As this is a very complex approach, in the present paper we shall focus on radon data only. We shall follow the Burnett model developed for estimation of SGD fluxes in coastal waters (Burnett and Dulaiova, 2003, 2006; De Oliveira et al., 2003).

We assume that radon may be advected via groundwater discharge into coastal water. On the basis of measured radon concentrations in coastal seawater we calculate radon inventories averaged over several hours. The radon flux  $F_{Rn}$  may be then expressed as

$$F_{Rn} = \frac{I_{Rn}}{\left(1 - \frac{\exp(-\lambda t)}{\lambda}\right)} \quad (3)$$

where  $I_{Rn}$  is the  $^{222}\text{Rn}$  inventory and  $\lambda$  is the  $^{222}\text{Rn}$  decay constant ( $7.54 \times 10^{-3} \text{ h}^{-1}$ ). After several  $^{222}\text{Rn}$  half-lives this equation reduces to  $\lambda I_{Rn}$ , and for the SGD flux  $F_{SGD}$  we can write

$$F_{SGD} = \frac{\lambda I_{Rn} - \lambda I_{Ra} + E \pm M}{C_{Rn}}, \quad (4)$$

where  $\lambda I_{Ra}$  is the production rate of  $^{222}\text{Rn}$  from  $^{226}\text{Ra}$ ,  $E$  is the atmospheric evasion of radon,  $M$  represents the horizontal mixing of radon, and  $C_{Rn}$  is the  $^{222}\text{Rn}$  concentration in the porewater. Several approximations have to be made for estimation of SGD fluxes from measured  $^{222}\text{Rn}$  concentrations:

- (1) The correction for supported radon was done by subtracting an equivalent activity of  $^{226}\text{Ra}$  measured in seawater close to the Base ( $8 \text{ Bq m}^{-3}$ ).
- (2) The average atmospheric evasion in Flamengo Bay was estimated to be  $0.8 \pm 0.5 \text{ Bq m}^{-2} \text{ h}^{-1}$  following the previous work of De Oliveira et al. (2003), and the more recent study of Burnett et al. (2008).
- (3) The losses due to mixing of SGD with offshore seawater were estimated to be  $12 \pm 9 \text{ Bq m}^{-2} \text{ h}^{-1}$  using data published by De Oliveira et al. (2003) and Burnett et al. (2008).

- (4) We expect that benthic fluxes of radon are driven mainly by groundwater (porewater) advection. The mean  $^{222}\text{Rn}$  concentration in porewater was estimated to be  $5.5 \text{ kBq m}^{-3}$  on the basis of measurements of Cable and Martin (2008), which were carried out at two sites (MS-3 and MS-5), close to our monitoring site (Fig. 3).

The estimated SGD fluxes from underwater gamma-spectrometry monitoring show similar patterns with time as the  $^{222}\text{Rn}$  concentrations presented in Fig. 9. The SGD fluxes varied during 22–26 November between 8 and  $40 \text{ cm d}^{-1}$  (the unit is  $\text{cm}^3/\text{cm}^2$  per day), with an average value of  $21 \text{ cm d}^{-1}$ . The obtained SGD flux is similar to that obtained between 16 and 20 November 2003 at Flamengo Bay by Burnett et al. (2008), who found values between 1 and  $29 \text{ cm d}^{-1}$  (average value  $13 \text{ cm d}^{-1}$ ). The SGD fluxes estimated at a nearby site MS-3 by Cable and Martin (2008) from porewater inventories ( $9\text{--}24 \text{ cm d}^{-1}$ ) and from artificial tracers ( $53 \text{ cm d}^{-1}$ ) are also in agreement with our values. Much larger SGD fluxes (up to  $300 \text{ cm d}^{-1}$ ) were measured at the low tide shoreline by manual and continuous seepage meters groups (Bokuniewicz et al., 2008; Taniguchi et al., 2008), however, comparable results with our data were obtained for a site situated about 10 m from the shoreline. Generally, these results showed large temporal and spatial variations in SGD fluxes observed in the small bay area.

Using the two end-members mixing model we estimated that at the monitoring site the contribution of fresh water in seawater varied between 4 and 20%, with an average value of 10%. However, with offshore distance, as documented by isotopic composition of collected samples, there was only a small contribution of fresh water in the submarine groundwater discharge.

## 6. Conclusions

Stable isotopes, tritium, radium isotopes, radon, trace elements and nutrients were analysed in several water samples from two campaigns carried out in the coastal region of Ubatuba, south-eastern Brazil, with the aim of investigating SGD in the area. The main observations made in this study may be summarised as follows:

- (1) The isotopic composition of submarine waters ( $\delta\text{D}$ ,  $\delta^{18}\text{O}$ ,  $^3\text{H}$ ) is characterised by significant variability and heavy isotope enrichment. The groundwater end-member can be represented by groundwater springs observed close to the Oceanographic Base. The stable isotopes and tritium data showed good separation of groundwater and seawater groups. The water samples from monitoring wells and seepage chambers were situated between the both main groups, representing mixtures of groundwater and seawater. The contribution of groundwater in submarine waters varied from a few % to 17%, depending on the location and the tide level.
- (2) Spatial distribution of  $^{222}\text{Rn}$  activity concentration offshore Ubatuba has revealed changes between 50 and

$200 \text{ Bq m}^{-3}$  which were in opposite relationship with observed salinities. Time series of  $^{222}\text{Rn}$  activity concentration in Flamengo Bay ( $1\text{--}5 \text{ kBq m}^{-3}$ ) confirmed a negative correlation between the  $^{222}\text{Rn}$  activity concentration and tide/salinity. The variations in  $^{222}\text{Rn}$  activity concentration were caused by sea level changes as tide effects induce variations of hydraulic gradients, which increase  $^{222}\text{Rn}$  concentration during lower sea level, and opposite, during high tides where the  $^{222}\text{Rn}$  activity concentration was smaller. A lower  $^{222}\text{Rn}$  activity concentration during high tides may also be due to a dilution of bay waters by offshore waters. At the monitoring site the contribution of fresh water in the seawater varied between 4 and 20%, with an average value of 10%.

- (3) The estimated SGD fluxes varied during 22–26 November between 8 and  $40 \text{ cm d}^{-1}$  (the unit is  $\text{cm}^3/\text{cm}^2$  per day), with an average value of  $21 \text{ cm d}^{-1}$ . These estimates were in a reasonable agreement with manual and continuous seepage meter measurements.
- (4) Radium isotope and nutrient data showed scattered distributions with salinity and distance offshore. This indicates that in the complex coast with many small bays and islands, the area has been influenced by local currents and groundwater–seawater mixing. Therefore, the sources of nutrients observed in the visited bays are both due to transport of pollutants by local currents and due to contributions from SGD.
- (5) Large changes in isotopic composition of seawater observed in a relatively small area document the importance of the isotopic characterization of coastal waters for better understanding of groundwater–seawater interactions in the region. SGD in the Ubatuba area is fed by coastal contaminated groundwater and re-circulated seawater (with different proportions of groundwater in the mixture), which gives rise to potential environmental concern with implications for the management of freshwater resources in the region.

## Acknowledgements

The authors would like to thank colleagues who participated in the 2002 and 2003 expeditions to Ubatuba for fruitful collaboration. We are grateful to Drs J. Cable and H. Bokuniewicz for providing water samples from piezometer multi-samplers and from seepage chambers, respectively. Three anonymous reviewers are acknowledged for useful comments. We also thank students Patrícia da Costa Lopes and Victor Gonzalez Chiozzinni, who assisted in sampling and analysis of  $^{222}\text{Rn}$ , Ra isotopes and nutrients. The Oceanographic Institute of the University of São Paulo, especially Dr Valdenir Veronese Furtado, is acknowledged for water level data and for logistical support during the field work. Captains and the crews (especially Mr Oziel, Mr Manuel and Mr Orlando) of the R/Vs Veliger II and Albacora are acknowledged for assistance during the oceanographic investigations. IPEN is acknowledged for logistical support during the field work. This research work was supported by International Atomic Energy

Agency, Research Contract no. 12151, and by Fundação de Amparo à Pesquisa no Estado de São Paulo, Process no. 2002/08154-9. The IAEA is grateful to the Government of the Principality of Monaco for the support provided to its Marine Environment Laboratories.

## References

- Aggarwal, P.K., Kulkarni, K.M., Povinec, P.P., Han, L.-F., Groening, M., 2004. Environmental isotope investigation of submarine groundwater discharge in Sicily, Italy. In: Book of Extended Synopses, IAEA-CN-118. IAEA, Austria, Vienna, pp. 222–223.
- Almeida, K.C.S., Oikawa, H., de Oliveira, J., Duarte, C.L., 2006. Degradation of petroleum hydrocarbons in seawater by ionizing radiation. *Journal of Radioanalytical and Nuclear Chemistry* 270, 93–97.
- Boehm, A.B., Paytan, A., Shellenbarger, G.G., Davis, K.A., 2006. Composition and flux of groundwater from a California beach aquifer: implications for nutrient supply to the surf zone. *Continental Shelf Research* 26, 269–282.
- Bokuniewicz, H., 1992. Analytical description of sub-aqueous groundwater discharge. *Estuaries* 15, 458–464.
- Bokuniewicz, H., Taniguchi, M., Ishitobi, T., Charette, M., Allen, M., Kontar, E.A., 2008. Direct measurements of submarine groundwater discharge (SGD) over a fractured rock aquifer in Flamengo Bay Brazil. *Estuarine, Coastal and Shelf Science* 76 (3), 466–472.
- Braga, E.S., Muller, T.J., 1998. Observation of regeneration of nitrate, phosphate and silicate during upwelling off Ubatuba, Brazil, 23°S. *Continental Shelf Research* 18, 915–922.
- Burnett, W.C., Dulaiova, H., 2003. Estimating the dynamics of groundwater input into the coastal zone via continuous radon-222 measurements. *Journal of Environmental Radioactivity* 69, 21–35.
- Burnett, W.C., Dulaiova, H., 2006. Radon as a tracer of submarine groundwater discharge into a boat basin in Donnalucata, Sicily. *Continental Shelf Research* 26, 862–873.
- Burnett, W.C., Chanton, J., Christoff, J., Kontar, E., Krupa, S., Lambert, M., Moore, W., O'Rourke, D., Paulsen, R., Smith, C., Smith, L., Taniguchi, M., 2000. Assessing methodologies for measuring groundwater discharge to the ocean. *EOS* 83, 117–123.
- Burnett, W.C., Taniguchi, M., Oberdorfer, J.A., 2001a. Assessment of submarine groundwater discharge into the coastal zone. *Journal of Sea Research* 46, 109–116.
- Burnett, W.C., Kim, G., Lane-Smith, D., 2001b. A continuous radon monitor for assessment of radon in coastal ocean waters. *Journal of Radioanalytical and Nuclear Chemistry* 249, 167–172.
- Burnett, W.C., Aggarwal, P.K., Aureli, A., Bokuniewicz, H., Cable, J.E., Charette, M.A., Kontar, E., Krupa, S., Kulkarni, K.M., Loveless, A., Moore, W.S., Oberdorfer, J.A., Oliveira, J., Ozyurt, N., Povinec, P.P., Privitera, A.M.G., Rajar, R., Ramessur, R.T., Scholten, J., Stieglitz, T., Taniguchi, M., Turner, J.V., 2006. Quantifying submarine groundwater discharge in the coastal zone via multiple methods. *The Science of the Total Environment* 367, 498–543.
- Burnett, W.C., Peterson, R., Moore, W.S., de Oliveira, J., 2008. Radon and radium isotopes as tracers of submarine groundwater discharge – results from the Ubatuba, Brazil SGD assessment intercomparison. *Estuarine, Coastal and Shelf Science* 76 (3), 501–511.
- Cable, J.E., Martin, J.B., 2008. In situ evaluation of nearshore marine and fresh porewater transport into Flamengo Bay, Brazil. *Estuarine, Coastal and Shelf Science* 76 (3), 473–483.
- Castro Filho, B.M., Miranda, L.B., Miyao, S.Y., 1987. Hydrographic conditions in the continental shelf off Ubatuba: seasonal and medium scale changes. *Boletim do Instituto Oceanografico* 35, 135–151.
- Coleman, M.L., Sheppard, T.J., Durham, J.J., Rouse, J.E., Moore, G.R., 1982. Reduction of water with zinc for hydrogen isotope analysis. *Analytical Chemistry* 54, 993–995.
- Craig, H., 1961. Isotopic variation in meteoric waters. *Science* 133, 1702–1703.
- De Oliveira, J., Burnett, W.C., Mazzilli, B.P., Braga, E.S., Farias, L.A., Christoff, J., Furtado, V.V., 2003. Reconnaissance of submarine groundwater discharge at Ubatuba coast, Brazil, using <sup>222</sup>Rn as a natural tracer. *Journal of Environmental Radioactivity* 69, 37–52.
- De Oliveira, J., Mazzilli, B.P., Teixeira, W.E., Sauer, C.H., Moore, W.S., Braga, E.S., Furtado, V.V., 2005. Determination of naturally occurring Ra isotopes in Ubatuba-SP, Brazil to study coastal dynamics and groundwater input. In: Méndez-Vilas, A. (Ed.), *Recent Advances in Multidisciplinary Applied Physics*. Elsevier, Amsterdam, Netherlands, pp. 805–824.
- De Oliveira, J., Charette, M., Allen, M., Braga, E.S., Furtado, V.V., 2006a. Coastal water exchange rate studies at the southeastern Brazilian margin using Ra isotopes as tracers. In: Povinec, P.P., Sanchez-Cabeza, J.A. (Eds.), *Radionuclides in the Environment*. Elsevier, Amsterdam, Netherlands, pp. 345–359.
- De Oliveira, J., Costa, P., Braga, E.S., 2006b. Seasonal variations of <sup>222</sup>Rn and SGD fluxes to Ubatuba embayments, São Paulo. *Journal of Radioanalytical and Nuclear Chemistry* 269 (3), 689–695.
- De Oliveira, J., Elísio, A.C.R., Teixeira, W.E., Peres, A.C., Burnett, W.C., Povinec, P.P., Somayajulu, B.L.K., Braga, E.S., Furtado, V.V., 2006c. Isotope techniques for assessment of submarine groundwater discharge and coastal dynamics in Ubatuba coastal areas, Brazil. *Journal of Coastal Research* SI39, 1084–1086.
- Epstein, S., Mayeda, T., 1953. Variation of O<sup>18</sup> content of waters from natural sources. *Geochimica et Cosmochimica Acta* 4, 213–224.
- Gonfiantini, R., 1978. Standards for stable isotope measurements in natural compounds. *Nature* 271, 534–536.
- Levy-Palomo, I., Comanducci, J.-F., Povinec, P.P., 2004. Investigation of submarine groundwater discharge in Sicilian and Brazilian coastal waters using underwater gamma-spectrometer. In: Book of Extended Synopses, IAEA-CN-118. IAEA, Austria, Vienna, pp. 228–229.
- Lopes, P.C., 2005. Estudo da variação sazonal das concentrações de <sup>222</sup>Rn em amostras de água do mar nas enseadas de Ubatuba, para a estimativa da descarga de águas subterrâneas. Dissertação de Mestrado na Área de Tecnologia Nuclear- Aplicações. Instituto de Pesquisas Energéticas e Nucleares, São Paulo, 77 pp. (in Portuguese).
- Mahiques, M.M., 1995. Sedimentary dynamics of the bays off Ubatuba, State of São Paulo. *Boletim do Instituto Oceanografico*. São Paulo 43 (2), 111–122.
- Martin, J., Cable, J., Swarzenski, P., Lindenberg, M., 2004. Enhanced submarine ground water discharge from mixing of porewater and estuarine water. *Ground Water* 42, 1001–1010.
- Mesquita, A.R., 1997. *Marés, Circulação e Nível do Mar na Costa Sudeste do Brasil*. Relatório Fundespa, São Paulo.
- Moore, W.S., 1996. Large groundwater inputs to coastal waters revealed by Ra-226 enrichments. *Nature* 380, 612–614.
- Moore, W.S., 2000. Ages of continental shelf waters determined from <sup>223</sup>Ra and <sup>224</sup>Ra. *Journal of Geophysical Research* 105, 22117–22122.
- Moore, W.S., 2006. Radium isotopes as tracers of submarine groundwater discharge in Sicily. *Continental Shelf Research* 26, 852–861.
- Moore, W.S., Arnold, R., 1996. Measurement of <sup>223</sup>Ra and <sup>224</sup>Ra in coastal waters using a delayed coincidence counter. *Journal of Geophysical Research* 101, 1321–1329.
- Moore, W.S., de Oliveira, J., 2008. Determination of residence time and mixing processes of the Ubatuba, Brazil, inner shelf waters using natural Ra isotopes. *Estuarine, Coastal and Shelf Science* 76 (3), 512–521.
- Moore, W.S., Wilson, A.M., 2005. Advective flow through the upper continental shelf driven by storms, buoyancy and submarine discharge. *Earth and Planetary Science Letters* 235, 564–576.
- Osvath, I., Povinec, P.P., 2001. Seabed gamma-ray spectrometry: applications at IAEA-MEL. *Journal of Environmental Radioactivity* 53, 335–349.
- Paytan, A., Shellenbarger, G.G., Street, J.H., Gonneea, M.E., Davis, K.A., Young, M.B., Moore, W.S., 2006. Submarine groundwater discharge: an important source of new inorganic nitrogen to coral reef ecosystem. *Limnology and Oceanography* 51, 343–348.
- Povinec, P.P., La Rosa, J., Lee, S.-H., Mulsow, S., Osvath, I., Wyse, E., 2001. Recent developments in radiometric and mass spectrometry methods for marine radioactivity measurements. *Journal of Radioanalytical and Nuclear Chemistry* 248, 713–718.

- Povinec, P.P., Ballestra, S., Gastaud, J., La Rosa, J., Lee, S.H., Liong Wee Kwong, L., Oregioni, B., Pham, M.K., 2002. Analytical Procedures and Quality Assurance Manual, Report 2/2002. IAEA-MEL, Monaco, 160 pp.
- Povinec, P., Aggarwal, P., Aureli, A., Burnett, W.C., Kontar, E.A., Kulkarni, K.M., Moore, W.S., Rajar, R., Taniguchi, M., Comanducci, J.-F., Cusimano, G., Dulaiova, H., Gatto, L., Hauser, S., Levy-Palomo, I., Ozorovich, Y.R., Privitera, A.M.G., Schiavo, M.A., 2006a. Characterisation of submarine ground water discharge offshore south-eastern Sicily – SGD Collaboration. *Journal of Environmental Radioactivity* 89, 81–101.
- Povinec, P.P., Comanducci, J.-F., Levy-Palomo, I., Oregioni, B., 2006b. Monitoring of submarine groundwater discharge along the Donnalucata coast in the south-eastern Sicily using underwater gamma-ray spectrometry of radon decay products. *Continental Shelf Research* 26, 874–884.
- Stieglitz, T., 2005. Submarine groundwater discharge into the near-shore zone of the Great Barrier Reef, Australia. *Marine Pollution Bulletin* 51, 51–59.
- Taniguchi, M., Burnett, W.C., Cable, J.E., Turner, J.V., 2002. Investigation of submarine groundwater discharge. *Hydrological Processes* 16, 2115–2129.
- Taniguchi, M., Stieglitz, T., Ishitobi, T., 2008. Temporal variability of water quality of submarine groundwater discharge in Ubatuba, Brazil. *Estuarine, Coastal and Shelf Science* 76 (3), 484–492.
- Teixeira, W.E., 2004. Determinação das concentrações dos isótopos naturais de rádio em amostras costeiras do litoral norte do Estado de São Paulo. Dissertação de Mestrado na Área de Tecnologia Nuclear-Aplicações. Instituto de Pesquisas Energéticas e Nucleares, São Paulo, 89 pp. (in Portuguese).
- Weinstein, Y., Less, G., Kafri, U., Herut, B., 2006. Submarine groundwater discharge in the Southeastern Mediterranean. In: Povinec, P.P., Sanchez-Cabeza, J.A. (Eds.), *Radionuclides in the Environment*. Elsevier, Amsterdam, pp. 360–372.